Atmospheric
Chemistry
and Physics
Discussions

Open Access

EGU

1   Potential impact of carbonaceous aerosols on the Upper Troposphere and

2   Lower Stratosphere (UTLS) during Asian summer monsoon in a global

3   model simulation

4   Suvarna Fadnavis[1], Gayatry Kalita[1], K. Ravi Kumar[1], Blaz Gasparini[2] and Jui-Lin Frank Li[3]

5   [1]Indian Institute of Tropical Meteorology, Pune, India

6   [2]Institute for Atmospheric and Climate Science, ETH Zürich, Switzerland

7   [3]Jet Propulsion Laboratory, California Institute of Technology, Pasadena, California

8   **Abstract**

9   Recent satellite observations show efficient vertical transport of Asian pollutants from the

10   surface to the upper level anticyclone by deep monsoon convection. In this paper, we

11   examine the transport of carbonaceous aerosols including Black Carbon (BC) and Organic

12   Carbon (OC) into the monsoon anticyclone using of ECHAM6-HAM, a global aerosol

13   climate model. Further, we investigate impacts of enhanced (doubled) carbonaceous aerosols

14   emissions on the UTLS from sensitivity simulations.

15   These model simulations show that boundary layer aerosols are transported into the monsoon

16   anticyclone by the strong monsoon convection from the Bay of Bengal, southern slopes of

17   the Himalayas and the South China Sea. Doubling of emissions of BC and OC aerosols, each,

18   over the South East Asia (10°S - 50°N; 65°E - 155°E) shows that lofted aerosols produce

19   significant warming in the mid/upper troposphere. These aerosols lead to an increase in

20   temperature by 1K - 3 K in the mid/upper troposphere and in radiative heating rates by 0.005

21   K/day near the tropopause. They alter aerosol radiative forcing at the surface by -1.4 W/m^2;

22   at the Top Of the Atmosphere (TOA) by +1.2 W/m^2 and in the atmosphere by 2.7 W/m^2 over

Atmospheric
Chemistry
and Physics
Discussions

23   the Asian summer monsoon region (20ºN - 40°N, 60ºE - 120°E). Atmospheric warming

24   increases vertical velocities and thereby cloud ice in the upper troposphere. An anomalous

25   warming over the Tibetan Plateau (TP) facilitate the relative strengthening of the monsoon

26   Hadley circulation and elicit enhancement in precipitation over India and north east China.

27   *Key words*: Aerosol radiative forcing; Black carbon and Organic carbon aerosols; ECHAM6-

28   HAM; Upper Troposphere and Lower Stratosphere (UTLS); Asian Tropopause Aerosol

29   Layer (ATAL).

30

1. Introduction

South East Asia ($10°$S–$50°$N; $65°$E–$155°$E) being one of the most fast-growing population and economies which contributes significantly to the emission of global aerosol particles (Ramanathan and Crutzen, 2003; Lin et al., 2013). India and China are the two major contributors in South East Asia (Carmicael et al., 2009; Lin et al., 2014; Butt et al., 2016). Black Carbon (BC) and Organic Carbon (OC) are the important aerosol species as they contribute largely to the climate forcing (Penner et al., 1998; Chung and Seinfeld, 2002; Ramanathan and Carmichael, 2008; Hodnebrog et al., 2014), alter the energy balance in the atmosphere and the global water cycle (Solomon et al., 2007). Recent studies show that their impacts on local meteorology and monsoon circulation are significantly large (Ackerman et al., 2000; Ramanathan et al., 2001a, 2001b; Lelieveld et al., 2001; Menon et al., 2002; Manoj et al., 2011). BC and OC together account for more than 60 % of the AOD (Chin et al., 2009; Streets et al., 2009).

There is ever growing concern for rapidly increasing anthropogenic emissions of carbonaceous aerosols namely BC and OC. Global emissions of BC have almost doubled during the past century (Baron et al., 2009). Developing countries in Asia, e.g. India and China produce BC emissions at high growth rates. These countries together produced about 40% of total world BC emissions from combustion (Kopp and Mauzerall, 2010). The estimated growth of BC is 46 % (33% in OC) over China and 41% (35% in OC) over India during 2000 to 2010 (Lu et al., 2011). On a regional scale, their emissions are high over densely populated Indo-Gangetic Plains in India and eastern China (Kumar et al., 2011; Lelieveld, 2001; Gautam et al., 2011; Fadnavis et al., 2013; Zhang et al., 2015) (see Fig. 1).

Atmospheric
Chemistry
and Physics
Discussions

54   Majority of BC and OC aerosols are formed by incomplete combustion (Satheesh and

55   Ramanathan; 2000; Carmicael et al., 2009). The important emission sources of BC aerosols are

56   diesel vehicles, exhaust from coal-based power plants, exhaust from industries, forest fires and

57   residential bio-fuel and fossil-fuel combustion. The OC aerosols are produced from fossil fuel

58   and biofuel burning and natural biogenic emissions. Biogenic carbonaceous aerosol consist of

59   plant debris, pollen, fungal spores, and bacteria (Jacobson et al., 2000; Bond et al., 2004) and

60   secondary organic aerosol from oxidation of volatile organic compounds (VOCs) (Solomon et

61   al., 2007).

62   Recent satellites, Cloud Aerosol Lidar and Infrared Path finder Satellite Observation

63   (CALIPSO) (Vernier et al., 2011; Thomason and Vernier, 2013), Stratospheric Aerosol and Gas

64   Experiment II (SAGE) (Thomason and Vernier, 2013) and Balloonsonde (Vernier, et al., 2015)

65   observations show Asian Tropopause Aerosol Layer (ATAL) near the tropopause persisting

66   during the monsoon season (June-September). Satellite observations reveal transport of trace

67   gasses (CO, PAN, H_2O HCN) into the upper level monsoon anticyclone by deep monsoon

68   convection (Park et al., 2009; Randel et al., 2010, Kunz et al.,2010; Ploeger et al., 2011; 2012;

69   2013; Fadnavis et al., 2014; 2015, Govardhan et al., 2017). Moreover, both back trajectory

70   analysis based on CALIOP observations (Vernier et al., 2015) and modeling studies (Fadnavis et

71   al., 2013) indicate that deep monsoon convection transports boundary layer aerosols into the

72   UTLS. A Civil Aircraft for Regular Investigation of atmosphere Based on an Instrument

73   Container (CARBIC) measurements show aerosols at the lower levels in the ATAL contain

74   higher levels of carbonaceous and sulfate aerosols. The ratio of carbon to sulfur is ~4.0 with

75   concentrations of carbon ~36 ng/m^3 and sulfur ~ 13 ng/m^3 in the Asian upper troposphere during

76   August 2006, 2007 and 2008 (Vernier et al., 2015). Carbonaceous aerosols in the upper

Atmospheric
Chemistry
and Physics
Discussions

77   troposphere lead to atmospheric heating due to their absorptive properties which may

78   subsequently alter the atmospheric thermal structure and cloud amounts. Higher concentrations

79   of carbonaceous aerosols in the ATAL may significantly alter thermal structure of the UTLS and

80   therefore the underlying monsoon circulation (Meehl et al., 2008; Kloster et al., 2009). The

81   ATAL may affect the radiative forcing regionally. Vernier et al., (2015) reported that the ATAL

82   had exerted a short-term regional forcing at the top of the atmosphere ~ -0.1 W/m^2 during past

83   two decades.

84   Asian Summer Monsoon (ASM) has a major impact on agriculture, water resources, and

85   economy and social life. Therefore it is important to study the impact of fast-growing Asian

86   emission of carbonaceous aerosols on monsoon precipitation. However, there are a few studies

87   reporting the impacts of carbonaceous aerosols on precipitation over India (Meehl et al., 2008;

88   Wang et al., 2009; Ganguly et al., 2012) and China (Guo et al., 2013; 2015). Since convective

89   transport (during the monsoon season) inter-links tropospheric processes with the UTLS (Randel

90   et al., 2010; Vogel et al., 2011, 2015; Fadnavis et al., 2013), it is essential to understand impacts

91   of boundary layer emissions on the UTLS. To our knowledge, transport of carbonaceous aerosols

92   from the boundary layer to upper troposphere, their impacts on the UTLS and connecting

93   monsoon circulation are not explored in detail. In this study, we address the question of the

94   impact of rapidly growing emissions of carbonaceous aerosols (BC and OC) on the thermal

95   structure of the UTLS, monsoon transport processes and rainfall over India and China. We

96   perform control and sensitivity simulations using the ECHAM6-HAM aerosol climate model. In

97   sensitivity experiment, we doubled anthropogenic emissions of BC and OC, each, over the South

98   East Asia (10°S-50°N; 65°E-155°E). The paper is organized as follows; in Section 2 model

99   simulations and satellite observations are described. The transport processes are discussed in

Atmospheric
Chemistry
and Physics
Discussions

100 Section 3. The impact of enhanced carbonaceous aerosols emissions on the UTLS and monsoon

101 precipitation are described in Section 4, followed by conclusions given in Section 5.

102 **2. Model simulations and satellite data analysis**

103 **2.1 Experimental setup and model simulations**

104 The fully coupled aerosol-climate model ECHAM6-HAM (version echam6.1.0-ham2.1-

105 moz0.8) used in this study comprises the general circulation model ECHAM6 (Stevens et al.,

106 2013) coupled to the aerosol sub-module Hamburg Aerosol Model (HAM) (Stier et al., 2005,

107 Zhang et al., 2012). HAM predicts the evolution of sulfate (SU), black carbon (BC), particulate

108 organic matter (POM), sea salt (SS), and mineral dust (DU) aerosols. The size distribution of

109 aerosol population being described by seven log-normal modes with prescribed variance as in the

110 M7 aerosol module (Vignati et al., 2004; Stier et al., 2005; Zhang et al., 2012). Moreover, HAM

111 uses the two-moment cloud microphysics scheme in which the nucleation scavenging of aerosol

112 particles by acting as cloud condensation nuclei or ice nuclei, freezing and evaporation of cloud

113 droplets and melting and sublimation of ice crystals is treated explicitly (Lohmann et al., 2007,

114 Lohmann et al., 2010, Neubauer et al., 2014). The anthropogenic and fire emissions of SO_2, BC,

115 and OC are based on the AEROCOM-ACCMIP-II emission inventory. The anthropogenic

116 emissions are based on Lamarque et al., (2010). The biomass burning emissions are from GICC

117 1850 - 1950 (Mieville et al., 2010), RETRO 1960-1990 (Schultz et al., 2008) and GFED v2

118 (1997 - 2008) (van der Werf et al., 2006). Biogenic emissions are derived from MEGAN

119 (Guenther et al., 1995) and fossil fuel sources are provided by the ACCMIP inventory

120 (Lamarque et al., 2010). In the model, biogenic OC is directly inserted via emissions. Secondary

121 organic aerosol (SOA) emissions are as described by Dentener et al. (2006). The emissions of

122   sea salt (Guelle et al., 2001 and Stier et al., 2005) and dust (Tegen et al., 2002; Cheng et al.,

123   2008) are computed interactively.

124   The model simulations are performed at the spectral resolution of T63. This spectral

125   representation is associated with a horizontal resolution of 1.875° x 1.875° on a Gaussian grid

126   and a vertical resolution of 47 levels spanning from the surface up to 0.01 hPa. The simulations

127   have been carried out at a time step of 20 minutes. AMIP sea surface temperature (SST) and sea

128   ice cover (SIC) are used as lower boundary conditions. Note that our base year for aerosol and

129   trace gas emissions is 2000. Each simulation was performed for the 30 years from January 1979

130   to December 2009. We analyze simulated data for 20 years (1989-2009) considering initial ten

131   years as spin-up time. Emissions are the same in each simulation, and meteorology varied

132   because of different monthly sea surface temperature (SST) and sea ice (SIC) data. Most of the

133   models underestimate BC and OC mass concentrations observed over Asia (Mao et al., 2011;

134   Bond et al., 2013; Butt et al., 2016; Winiger et al., 2016). Bond et al. (2013) have suggested that

135   global atmospheric absorption attributable to black carbon is too low in many models and should

136   be increased by a factor of three. Butt et al. (2016) obtained better predictions when residential

137   carbonaceous emissions were doubled. We performed control experiment (CTRL) in which we

138   kept our emissions at the baseline levels (the year 2000) and a sensitivity experiment (DEMISS)

139   in which we doubled emissions of BC and OC, over the South East Asian region (65°E - 155°E;

140   10°S - 50°N). We compare CTRL simulation with DEMISS and analyze the impacts of doubled

141   carbonaceous emissions (BC and OC together) on the UTLS and rainfall during ASM season

142   (June - September).

143

144

2.2 Satellite measurements

2.2.1 The Tropical Rainfall Measuring Mission (TRMM)

The Tropical Rainfall Measuring Mission (TRMM) is a joint National Aeronautics and Space Administration (NASA) - Japan Aerospace Exploration (JAXA) satellite mission to monitor the tropical and subtropical precipitation and estimate its associated latent heat. TRMM was launched in 1997 from Tanegashima space center in Japan. The rainfall measuring instruments on the TRMM satellite include an electronically scanning radar Precipitation Radar (PR), (operating at 13.6 GHz), TRMM microwave image (TMI), a 9 channel passive microwave radiometer (which records radiation at the 10.65, 19.35, 37.0, 85.5 (V and H) and 21.3 (V) GHz), and Visible and Infrared Scanner (VIRS) with five operating channels (Kummerow et al., 1998). The 3B42 algorithm produces TRMM adjusted merged infrared precipitation rate and root mean square (RMS) precipitation error estimates (Huffmen et al., 2007). The algorithm combines multiple independent precipitation estimates from the TMI, Advanced Microwave Scanning Radiometer for Earth Observing Systems (AMSR-E), Special Sensor Microwave Imager (SSMI), Special Sensor Microwave Imager/Sounder (SSMIS), Advanced Microwave Sounding Unit (AMSU), Microwave Humidity Sounder (MHS), and microwave-adjusted merged geo-infrared (IR). The final 3B42 precipitation (in mm hr^{-1}) estimates have a 3-hourly temporal resolution and a 0.25-degree by 0.25-degree spatial resolution. TRMM precipitation can be obtained from https://disc2.gesdisc.eosdis.nasa.gov/data/TRMM_L3/TRMM_3B42.7/. 3-hourly precipitation data are averaged to obtain daily mean. Then, seasonal mean (June-September) is computed from daily mean data. Further, seasonal mean data is averaged for 20 years (1997-2016) to obtain climatology of the monsoon season.

2.2.2 CloudSat and Cloud-Aerosol Lidar Infrared Pathfinder Satellite Observations (CALIPSO)

Cloud–Aerosol Lidar and Infrared Pathfinder Satellite Observation (CALIPSO) and CloudSat are two A-Train constellation satellites, launched together in April 2006. They provide information related to the role of cloud and aerosol in the Earth's climate system and radiative imbalance of the atmosphere. The Cloud Profiling Radar (CPR) on board of CloudSat satellite is a 94-GHz nadir-looking radar which measures the power backscattered by clouds as a function of distance. It provides information on cloud abundance, distribution, structure, and radiative properties (Stephens et al., 2008). The Cloud-Aerosol Lidar with Orthogonal Polarization (CALIOP) is an elastically backscattered active polarization sensitive Lidar instrument onboard CALIPSO. The CALIOP transmit laser light simultaneously at 532 nm and 1064 nm at a pulse repetition rate 20.16Hz. The Lidar receiver subsystem measures backscatter intensity at 1064 nm and two orthogonally polarized components of 532 nm backscatter signal that provides the information on the vertical distribution of aerosols and clouds, cloud particle phase, and classification of aerosol size (Winker et al., 2010; Powel et. al., 2013). In this study, we use Ice water content (IWC) dataset from the combined measurement of CloudSat and Calipso (2C-ICE_L3_V01) for the period 2007-2010. The 2C-ICE cloud product is an ice cloud retrieval derived from the combination of the CloudSat radar and CALIPSO Lidar, using a variational method for retrieving profiles of the IWC in ice clouds (Deng et al., 2013). The details of the data retrieval method are explained in Li et al., (2012). IWC data has been averaged for the monsoon season and period 2007-2010 to obtained seasonal climatology.

Atmospheric
Chemistry
and Physics
Discussions

2.3 Comparison with measurements

190

191   We compare CTRL simulated BC concentrations with in-situ measurements reported by

192   Babu et al., (2011) over Hyderabad (17º.48' N; 78º.40'E) in India on 17 March 2010 during pre-

193   monsoon season. Babu et al., (2011) obtained BC measurements using aethalometer installed in

194   the hydrogen-inflated balloon. For comparison, monthly mean simulated BC concentrations for

195   March are extracted at the grid centered at 17ºN, 78ºE. Figure 2a shows the comparative analysis

196   of model simulated BC and in situ measurements of BC. It can be seen that peaks near 4 km and

197   8.5 km are not reproduced by the model simulations. Balloon borne measurements show high

198   values of BC concentrations ~12 μg m^{-3} near 4-5 km altitude whereas the model simulations

199   show values of ~0.4-1 μ gm^{-3}. These peaks and fluctuation in BC profile indicate an influence of

200   meteorology on that day. The model could not reproduce such peaks as simulations were not

201   forced by the meteorology; while we show a monthly mean profile (model output is written at

202   every month). It must be mentioned that the vertical profile of simulated BC is over a wider

203   spatial grid (1.8º x 1.8º) whereas balloonsonde measurements by Babu et. al., (2011) are at a

204   single station. The model underestimates BC concentrations by ~2.1 μg m^{-3} near 2 km - 4 km

205   and ~0.8 μg m^{-3} near 6 km -7.5 km. Tripathi et al. (2007) reported BC concentrations ~8 μg m^{-3} -

206   4 μg m^{-3} between the surface to 2 km at Kanpur (80º.20'E, 26º.26'N). Simulated BC

207   concentrations at Kanpur show similar values (7.5 μg m^{-3} - 3 μg m^{-3}).

208   Figures 2b and 2c show the vertical distribution of cloud ice obtained from CTRL simulation and

209   climatology of seasonal mean from combined measurement of CloudSat and CALIPSO (2C-

210   ICE) (2007-2010) respectively, averaged for the monsoon season (June-September) and ASM

211   region (60ºE - 110º E;15ºN - 40ºN). It can be seen that simulated (3 mg/kg -10 mg/kg) and

212   observed cloud ice (5 mg/kg - 17 mg/kg), both, show high amounts in the upper troposphere (450

Atmospheric
Chemistry
and Physics
Discussions

213 hpa - 200 hPa) over the ASM region. The model simulations show maximum (7 mg/kg - 10

214 mg/kg) at ~350 hPa - 250 hPa over 80ºE - 100ºE while satellite observations (12 mg/kg – 17

215 mg/kg) show it at ~450 hPa-200 hPa over ~80ºE - 120ºE. These differences may be related to

216 uncertainties in satellite observations (Deng et al., 2010) and model biases, e.g., the model does

217 not consider large ice particles unlike the cloud ice measurement from CloudSat and CALIPSO.

218 The total ice water mass estimate from 2C-ICE, combine measurements from CALIPSO Lidar

219 depolarization which is sensitive to small ice particle (i.e., cloud ice represented in GCMs) while

220 CloudSat radar which is very sensitive to larger ice particles (i.e., precipitating ice or snow). In

221 most global climate models including all the CMIP3 and most of the CMIP5, only small particles

222 (i.e., cloud ice) are represented prognostically. The mass of large ice particles (about two-third of

223 total ice) and their radiative effects, however, are not included (e.g., Li et al., 2012; 2013).

224 We compare simulated (CTRL) seasonal mean (June-September) precipitation with TRMM

225 precipitation climatology (1997-2016). Figures 2d and 2e show the distribution of precipitation

226 as obtained from CTRL simulation and TRMM respectively. It can be seen that general spatial

227 pattern of precipitation simulated by the model is in good agreement with the TRMM. The model

228 could reproduce high amounts of precipitation over the Bay of Bengal, the South China Sea, and

229 the Western Ghats, in agreement with a numbers of past studies (Kang et al., 2002; Wang and

230 Linho, 2002; Zveryaev and Aleksandrova, 2004; Hirose and Nakamura, 2005; Xie et a.l., 2007;

231 Takahashi, 2016). However, model underestimates the rainfall over northern India and the

232 Western coast of India by ~ 2 mm/day - 10 mm/day and overestimates over the Tibetan Plateau

233 (TP) and the South China Sea by ~5 mm/day - 12 mm/day. It may be related uncertainties in

234 emissions, transport errors, and model coarse resolution.

235

Atmospheric
Chemistry
and Physics
Discussions

Open Access

EGU

3. Transportation of aerosol to the UTLS

236

237   Figure 3a depicts the vertical distribution of carbonaceous aerosols averaged over North

238   India (75ºE - 100ºE; 25ºN - 45ºN) during the annual cycle as obtained from CTRL simulation. It

239   shows elevated levels of aerosols (BC and OC together) from the surface to the tropopause

240   during pre-monsoon (March-May) and monsoon seasons. It shows a layer of carbonaceous

241   aerosols (~5 ng/m^3) in the upper troposphere ~170hPa - 100hPa. A layer of aerosols in the upper

242   troposphere is also observed by satellite (SAGE II, CALIPSO) and ground-based Lidar

243   measurements during the monsoon season (Vernier et al., 2011; Thomason and Vernier, 2013;

244   Fadnavis et al. 2013; He et al., 2014). Over the TP this aerosol layer extends above the

245   tropopause (18-19 km) (He et al., 2014).

246   A prominent feature in the UTLS over the ASM region during the summer season is a

247   large anticyclone. Satellite observations show a persistent maximum in trace gases (CO, H_2O,

248   PAN, HCN, CH_4, etc) (Li et al., 2005a; Randel and Park 2006, Fu et al., 2006; Park et al., 2008;

249   2009, Randel et al., 2010; Fadnavis et al., 2013, 2014, 2015) and aerosols (Tobo et. al., 2007;

250   Vernier et. al., 2011; Thomason and Vernier, 2013; Yu et al., 2015) in the ASM anticyclone.

251   Figure 3b exhibits the distribution of seasonal (June-September) mean carbonaceous aerosols

252   (BC and OC together) from CTRL simulation in the anticyclone (~100 hPa). In agreement with

253   previous studies (Tobo et. al., 2007 Vernier et. al., 2011), Fig. 3b also shows confinement of high

254   carbonaceous aerosols concentration (>5 ng/m^3) within the anticyclone. The wind vector at

255   100hPa depicts the extent of the anticyclone (20°E-120°E and 15°N-40°N).

256   Previous studies from model simulations and trajectory analysis show that rapid transport

257   of trace gases and aerosols from Asian boundary layer into the anticyclone is closely linked with

258   the deep ASM convection (Li et al, 2005; Randel and Park, 2006; Park et al., 2007; Park et al,

Atmospheric
Chemistry
and Physics
Discussions

259   2009; Xiong et al., 2009; Fadnavis et al, 2013, 2014 , 2015). We plot longitude-pressure and

260   latitude-pressure cross sections of carbonaceous aerosol from CTRL simulations to understand

261   their transport. Figure 3c displays seasonal mean longitude-pressure variation of carbonaceous

262   averaged over 15°N-35°N, along with wind vectors. It indicates that they are lifted up from the

263   Bay of Bengal, Indo-Gangetic Plains (70°E-90°E) and South China Sea (110°E-130°E) into the

264   anticyclone increasing the aerosol concentration to 4-6 ng/m^3 in the UTLS (above 200hPa)

265   across 40°E-110°E. Transport from southern slopes of Himalaya is evident in Figs. 3d. Figures

266   3e and 3f show the condensed cloud water (both liquid and ice). Its maxima point out areas of

267   frequent deep convective activity over the Bay of Bengal and the South China Sea (Fig. 3e) and

268   the southern flanks of the Himalayas (Fig. 3f). Thus transport of carbonaceous aerosols (seen in

269   Figs. 3c and 3d) from these regions into the upper level anticyclone may be due to deep monsoon

270   convection. Pollution transport (CO, HCN, NOX, PAN) from the Asian region to the UTLS due

271   to monsoon convection is also reported by Park et al. (2007), Randel et al. (2010), Fadnavis et

272   al., (2014, 2015). Figures 3c and 3d show that a fraction of aerosols crosses the tropopause and

273   enters into the lower stratosphere. It may be due to large scale upward motion within the

274   anticyclone shown by the wind vectors. Recently, trajectory analysis showed that air masses

275   within the anticyclone are transported into the lower stratosphere in the northern subtropics

276   (Garny and Randel, 2016).

277   We analyze the vertical profile of anomalies of carbonaceous aerosols obtained from a

278   difference between DEMISS and CTRL simulations. Longitude-pressure and latitude-pressure

279   cross sections of the anomalies are shown in Figs. 4a and 4b respectively. Enhanced anomalies

280   are seen along the transport pathways, e.g., from the Bay of Bengal, the South China Sea and

281   southern flanks of the Himalayas into the anticyclone. They show an enhancement of nearly 4

282   ng/m^3 relative mass of aerosol near the tropopause and part of it (>2 ng/m^3) enters the lower

283   stratosphere.

284   **4. Impact of enhanced carbonaceous aerosols emissions**

285   **4.1 Impact on radiative forcing and heating rates**

286   BC and OC aerosols absorb and scatter radiation, resulting in heating of the atmosphere

287   and reduction of solar radiation reaching the Earth's surface (Penner et al., 1998). The global

288   mean estimated cumulative (since 1970) BC radiative effect is +0.3 W/m^2 while OC emitted

289   from fossil fuels is estimated to be -0.1 W/m^2 (Myhre et al., 2013). The presence of BC aerosols

290   can change the sign of forcing from negative to positive (Haywood and Shine, 1997).

291   The convectively transported carbonaceous aerosols may alter radiative forcing, heating

292   rates, temperature, and vertical velocities in the UTLS. The carbonaceous aerosol can affect the

293   radiative energy balance of the atmosphere directly by scattering and absorbing solar radiation

294   and indirectly by acting as cloud condensation nuclei (Rosenfield 2000). This indirect forcing is

295   neglected in our model simulations as these aerosols are not considered to act as cloud

296   condensation nuclei. Anomalies in aerosol forcing estimated from DEMISS simulation against

297   CTRL (i.e., DEMISS - CTRL) are averaged for the monsoon season and ASM region (see Table-

298   1). Seasonal mean anomaly of aerosol forcing is +1.2 W/m^2 at the top of the atmosphere (TOA)

299   and -1.4 W/m^2 at the surface. The atmospheric radiative forcing is computed from the difference

300   between forcing at TOA and surface. The resultant anomaly of atmospheric aerosol radiative

301   forcing is ~2.6 W/m^2. It represents the energy trapped in the atmosphere due to the presence of

302   higher amounts of carbonaceous aerosols. Babu et al., (2002) reported BC radiative forcing +5

303   W/m^2 at the TOA and at the surface -23 W/m^2 in Bangalore (13ºN, 77ºE), India. Badarinath and

Atmospheric
Chemistry
and Physics
Discussions

304   Latha, (2006) obtained BC radiative forcing of +9 W/m^2 at the TOA and -33 W/m^2 at the surface

305   at Hyderabad (78ºE, 17ºN), India.

306   The resulting shortwave plus longwave atmospheric forcing due to doubled carbonaceous

307   aerosol will translate to a significant atmospheric heating (Babu et al., 2002). We obtained

308   anomalies in total heating rates (HR) due to carbonaceous aerosols (DEMISS - CTRL). Figures

309   4c and 4d show longitude-pressure (averaged for 15ºN-35ºN) and latitude-pressure (averaged for

310   80ºE-110ºE), cross sections of HR anomalies during the monsoon season (wind anomalies are

311   plotted over HR anomalies). Enhanced carbonaceous aerosols emissions increase HR near the

312   surface. High emissions from Indo-Gangetic Plains (70ºE - 90ºE, 25ºN - 35ºN) cause anomalous

313   heating (0.05 K/day) in the lower troposphere (1000 hPa - 600 hPa). Positive anomalies of HR

314   can be seen along the pathway through which carbonaceous aerosols are transported into the

315   anticyclone. It can be seen that carbonaceous aerosols have increased HR by ~0.003 K/day -

316   0.005 K/day at tropopause level in the AMS region in comparison with CTRL simulations (0.006

317   K/day - 0.01 K/day). Park et al. (2007) estimated net HR rates near the tropopause (averaged

318   over 60°E-150ºE) ~0.2 K/day - 0.6 K/day during the monsoon season. In comparison, HR

319   estimated from CTRL simulation ~ are less (0.1 K/day – 0.25 K/day) over the same region.

320   Radiative heating of the tropopause region increases the vertical motion and transport into the

321   lower stratosphere (Gettleman et al., 2004). Carbonaceous aerosols enhancement (> 2 ng/m^3) in

322   the lower stratosphere seen in Figs. 4a and 4b may be due to increase in vertical motion in

323   response to enhanced aerosol HR. This indicates that aerosols induce positive feedback in

324   vertical transport.

325

326

Atmospheric
Chemistry
and Physics
Discussions

4.2   Impact on temperature and precipitation

327

328   Further, we analyze changes in temperature induced by doubled carbonaceous aerosol

329 emissions. Figures 4e and 4f show the longitude-pressure (averaged over 15ºN - 35ºN) and

330 latitude-pressure (averaged over 60°E - 110°E) cross sections of temperature anomalies. These

331 aerosols induce significant warming in the mid-troposphere (500 hPa -300 hPa) over the ASM

332 region and a striking warm core like feature of anomalous warming (~3K) in the mid-upper

333 troposphere over the TP (70ºE - 90ºE, 30ºN - 45ºN) (Fig. 4f). The warm core over the TP plays

334 an important role in enhancing the ASM circulation (Flohn 1957; Yanai et al., 1992; Meehl,

335 1994; Li and Yanai, 1996; Wu and Zhang, 1998) (discussed later in this section). Figure 4e

336 shows cooling near the tropopause in the anticyclone with a small patch of positive anomalies

337 over the TP (80º-100°E). During the monsoon season, cold temperatures in the UTLS overlie

338 warm mid-troposphere (Randel and Park 2006; Park et al., 2007). Our model simulations show

339 that doubling of carbonaceous aerosol emissions amplifies the mid-tropospheric warming and

340 cooling near the tropopause.

341   During Northern hemispheric summer, heating over the TP maintains a large-scale

342 thermally driven vertical circulation (Yanai et al., 1992). The analysis of simulated vertical

343 velocities shows that carbonaceous aerosols induce positive anomalies over the southern TP and

344 Indo-Gangetic plains (Figs 5a and 5b). Thus carbonaceous aerosols amplify warming (Fig. 4e

345 and Fig. 4f) and enhance ascending motion over these regions. Previous studies (Rajagopalan

346 and Molnar, 2013, Vinoj et al., 2014) have reported that the warm ascending air above the TP

347 gradually spreads southward and descends over the northern Indian Ocean. The south-westerly

348 winds at the surface, on the other hand, complete the monsoon Hadley cell. This local circulation

349 system releases latent heat and further maintains the Tibetan warm core. Thus heating over the

350   TP leads to increased Indian summer monsoon rainfall by enhancing the cross-equatorial

351   circulation and concurrently strengthening both the Somali Jet and the westerly winds that bring

352   rainfall to India. Goswami et al., (1999) also reported that there is a strong correlation between

353   monsoon Hadley circulation and precipitation. Figure 5c shows that carbonaceous aerosols

354   strengthen the monsoon Hadley circulation, ascending motion over 10ºN - 20ºN and descending

355   over 0º-10ºS.

356   Thus Figs. 4a-4f and Figs 5a-5c suggest that enhanced emissions of carbonaceous

357   aerosols increase the HR, and amplify warm anomalies in the middle troposphere and cold

358   anomalies near the tropopause. Aerosol induced warming elicits enhancement in vertical

359   velocities. These aerosols induce an anomalous warming over the TP which in turn strengthens

360   the monsoon Hadley circulation. Previous studies (Meehl et al., 1994; Krishnamurthy and

361   Achuthavarier 2002) have explained the mechanism of strengthening of the monsoon Hadley

362   circulation facilitate enhanced precipitation over the Indian region. Consequently, aerosol

363   (carbonaceous) induced precipitation anomalies are positive over the Indian region (1 mm/day - 4

364   mm/day) (Fig. 5d). Strong positive anomalies (2 mm/day - 3.5 mm/day) are located over North

365   India, the Bay of Bengal, Western coast of India and foothills of Himalaya. There is an

366   enhancement in precipitation over North east China (0.2 mm/day - 2 mm/day) and some parts of

367   central and south China (0.2 mm/day - 1 mm/day). In agreement with the present study, aerosol-

368   climate modeling studies by Wang et al., (2004, 2007) also show enhancement in Indian summer

369   monsoon precipitation due to black carbon direct radiative forcing. Increases the Indian summer

370   monsoon precipitation due to the loading of absorbing aerosol (BC and dust) has been reported

371   in the past (Lau and Kim., 2006; Vinoj et al., 2014; Fadnavis et al., 2016). However, a mix

372   response is portrayed by Ganguly et al. (2012). Their ocean-atmosphere coupled model show

Atmospheric
Chemistry
and Physics
Discussions

373   reduction in precipitation over the western coastline of the Indian peninsula and increase over

374   north western part of Indian subcontinent. Reduction in precipitation is attributed to

375   anthropogenic local and remote aerosols. These differences may be due to different model-set

376   up, present study gives impact of doubled Asian carbonaceous aerosol emissions using Aerosol-

377   atmosphere-climate model. While, Ganguly et al. (2012) reports response of all anthropogenic

378   and biomass burning aerosols using a coupled atmosphere-slab ocean model simulations.

379   **4.3 Impact on water vapor, cloud ice**

380   Recently from satellite observations, Park et al., (2007) have shown that water vapor in

381   the upper troposphere (~216 hPa) varies coherently with deep monsoon convection both

382   temporally and spatially. Transport of high water vapor in the UTLS by the monsoon convection

383   has been reported in the past (Randel et al., 2001; Gettelman et al., 2004; Dessler and Sherwood,

384   2004; Fu et al., 2006; Randel and Park, 2006, Braesicke et al., 2011; Ploeger et al., 2013). We

385   analyze the difference in water vapor anomalies (DEMISS - CTRL) to understand the impact of

386   doubled Asian carbonaceous aerosol emissions on the transport of water vapor in the UTLS.

387   Figures 6a and 6b show an increase in water vapor transport in the upper troposphere and lower

388   stratosphere (0.1 ppmv - 2 ppmv). Water vapor anomalies ~8 ppmv - 20 ppmv are seen near 200

389   hPa and ~0.1 ppmv - 0.8 ppmv near the tropopause. Fadnavis et al. (2013) reported an increase

390   in water vapor (~ 0.1 ppmv - 10 ppmv) in the UTLS in response to increasing in aerosols which

391   are in agreement with the current study. In the past, Gettelman et al. (2004), Fu et al. (2006),

392   Fadnavis et al., (2013), Garny and Randel (2016) also reported transport of water vapor above

393   the tropopause into the lower stratosphere during the monsoon season. Enhanced aerosol

394   emissions increase water vapor transport into the lower stratosphere by enhancing heating rates,

395   mid/upper tropospheric warming, and vertical velocities.

Atmospheric
Chemistry
and Physics
Discussions

396   In addition to thermal and dynamical impact, aerosols in the UTLS also largely influence

397   the formation and microphysical properties of cirrus clouds. Cirrus clouds have a great impact on

398   radiation and intensity of the large-scale tropical circulation (Randall et al., 1989; Ramaswamy

399   and Ramanathan, 1989; Liu et al., 2003). Figures 6c - 6f show longitude-pressure and latitude-

400   pressure cross sections of anomalies of cloud ice and Ice Crystal Number Concentration (ICNC).

401   These figures show enhancement of anomalies of cloud ice (by 0.4 mg/m^3 - 1 mg/m^3) and ICNC

402   (by 0.08 1/mg) occurrence in the upper troposphere (350 hPa - 100 hPa). Maximum increase

403   (cloud ice by 0.6 mg/m^3 and ICNC by 0.08 m^{-3}) is seen in the 20ºN - 30ºN where stronger

404   upwelling motion prevails (Figs. 6d and 6f). A fraction of positive anomalies of ICNC are seen

405   near the tropopause indicating entrainment into the lower stratosphere. Positive anomalies in

406   cloud ice and ICNC (in the upper troposphere) may be due to enhancement in ASM deep

407   convection (increase in heating rates, mid/upper tropospheric temperature, vertical velocity, and

408   monsoon Hadley circulation) induced by the doubling of carbonaceous aerosols emissions.

409   **5. Conclusions**

410   In this paper, we investigated impacts of enhanced Asian (65°E - 155°E; 10°S - 50°N)

411   carbonaceous aerosols on the UTLS, underlying monsoon circulation and precipitation over

412   India and China using a state of the art aerosol-climate model. We performed sensitivity

413   experiments for doubling of carbonaceous aerosol over the Asian region.

414   To validate the model simulations, we compare simulated BC vertical profile with observations

415   from aethalometer launched on Balloonsonde at Hyderabad (78ºE, 17ºN) on 17 March 2010 in

416   pre-monsoon season; seasonal mean of simulated cloud ice content with climatology of

417   combined measurements from CloudSat and CALIPSO (2007-2010); and simulated precipitation

418   with climatology of TRMM observations (1997-2016). Comparison of the simulated vertical

Atmospheric
Chemistry
and Physics
Discussions

419   profile of BC aerosols with the balloon borne aethalometer measurements at Hyderabad (17

420   March 2010), shows that the model underestimates BC concentrations by ~2.1 μg m^{-3} ~0.8 μg m^{-}

421   ^{3} in the troposphere (4-8 km) during the pre-monsoon season. The spatial patterns of the

422   simulated season mean (June - September) precipitation are comparable with climatology of

423   TRMM precipitation (1997-2016) and cloud ice with combined measurements from CloudSat

424   and CALIOP (2007-2010) respectively. Simulated cloud ice is underestimated 2 mg/kg - 7 mg/kg

425   in the UTLS (60°E - 120°E; 15°N - 40°N) during the summer monsoon season.

426   Our model simulations show that monsoon convection over the Bay of Bengal, the South

427   China Sea and Southern flanks of the Himalayas transport Asian carbonaceous aerosol into the

428   UTLS. A persistent maximum of carbonaceous aerosols is seen within the anticyclone

429   throughout the ASM season, and a fraction of these aerosols enter the lower stratosphere.

430   Doubling emissions of carbonaceous aerosol over the Asian region leads to their enhancement

431   (by 4-6 ng/m^3) in the UTLS. They alter aerosol radiative forcing at the surface by -1.4 W/m^2; at

432   the TOA by +1.2 W/m^2 and in the atmosphere by 2.7 W/m^2. Positive anomalies of heating rates

433   are seen along the pathway through which aerosols are transported into the anticyclone. These

434   carbonaceous aerosols increase heating rates in the anticyclone (~100 hPa) by 0.003 K/day to

435   0.005 K/day. They induce significant warming (temperature increases by 1-3K) in mid/upper

436   troposphere over the ASM region. An anomalous in-atmospheric warming enhances vertical

437   velocities and thereby cloud ice (by 0.4-1 mg/m^3), ICNC (by 0.08 1/mg). A significant increase

438   in water vapor transport in the upper troposphere (0.5-10 ppmv) and lower stratosphere (0.1

439   ppmv - 0.5 ppmv) is apparently related to the mid/upper tropospheric warming. Doubling of

440   carbonaceous aerosols emissions enhance warming over the TP (~3K) and amplify cold

441   anomalies near the tropopause (-0.1K - -1K). An anomalous warming over the TP enhances the

Atmospheric
Chemistry
and Physics
Discussions

442 monsoon Hadley circulation and elicits an enhancement in precipitation over India (1-4 mm/day)

443 and eastern China (0.2 mm/day - 2 mm/day). In agreement with the present study, aerosol-

444 climate modeling studies by Wang et al., (2004, 2007) also show enhancement in Indian summer

445 monsoon precipitation due to black carbon direct radiative forcing. Observational evidences also

446 show that heavy loading of absorbing aerosols (BC and Dust) over the Indian subcontinent

447 facilitate enhancement of monsoon rainfall over India (Lau and Kim, 2006; Vinoj et al., 2014).

448 However, a mixed response, a regional increase (North western India) /decrease (Indian

449 Peninsula and eastern Nepal) in precipitation in response to anthropogenic and biomass burning

450 aerosol emissions is reported by Ganguly et al., (2012). These results differ from the present

451 study. It may be due to different model-set up, present study gives impact of doubled Asian

452 carbonaceous aerosol emissions using Aerosol-atmosphere-climate model. While, Ganguly et al.

453 (2012) reports response of all anthropogenic and biomass burning aerosols using a coupled

454 atmosphere-slab ocean model simulations.

455 We note that a realistic future emission scenario includes also increasing emissions of

456 sulfate aerosols and the response of climate and circulation to increasing CO_2 concentrations,

457 which might interplay with the presented results and lead to different dynamical and climatic

458 responses. Moreover, in future, we propose to re-evaluate the studies by using an aerosol model

459 coupled to the interactive chemistry, microphysics, the regional model with a better resolution of

460 the complex orography over Himalayas/TP, etc. Notwithstanding this, the work provides

461 valuable insight into the influence of growing Asian carbonaceous aerosols emissions on the

462 UTLS, connecting monsoon processes and precipitation in the Asian summer monsoon region.

463

Atmospheric
Chemistry
and Physics
Discussions

Open Access

EGU

467

Atmospheric
Chemistry
and Physics
Discussions

468   **References:**

469

472   Ackerman, A. S., Toon, O.B., Stevens, D.E., Heymsfield, A.J., Ramanathan,V., Welton, E, J.:
473   Reduction of tropical cloudiness by soot, Science, 288, 1042-1047, doi:
474   10.1126/science.288.5468.1042, 2000.

477   Babu, S. S., K. K. Moorthy, R. K. Manchanda, P. R. Sinha, S. K. Satheesh, D. P. Vajja, S.
478   Srinivasan, V. H. A. Kumar.: Free tropospheric black carbon aerosol measurements
479   using high altitude balloon: Do BC layers build "their own homes" up in the
480   atmosphere?, Geophys. Res. Lett., 38, L08803, doi:10.1029/2011GL046654, 2011.

483   Babu, S. S., S. K. Satheesh, and K. K. Moorthy.: Aerosol radiative forcing due to enhanced black
484   carbon   at   an   urban   site   in   India,   Geophys.   Res.   Lett.,   29,   1880,
485   doi:10.1029/2002GL015826, 2002.

486   Bond, T. C., Streets, D. G., Yarber, K. F., Nelson, S. M., Woo, J.-H., and Klimont, Z.: A
487   technology-based global inventory of black and organic carbon emissions from
488   combustion, J. Geophys. Res., 109, D14203, doi:10.1029/2003JD003697, 2004.

491   Bond, T.C., S. J. Doherty, D. W. Fahey, P. M. Forster,T. Berntsen, B. J. DeAngelo, M. G.
492   Flanner, S. Ghan, B. Kärcher, D. Koch, S. Kinne, Y. Kondo, P. K. Quinn, M. C. Sarofim,
493   M. G. Schultz, M. Schulz, C. Venkataraman, H. Zhang, S. Zhang, N. Bellouin, S. K.
494   Guttikunda, P. K. Hopke, M. Z. Jacobson, J. W. Kaiser, Z. Klimont, U. Lohmann, J. P.
495   Schwarz, D. Shindell, T. Storelvmo, S. G. Warren, and C. S. Zender.: Bounding the role
496   of black carbon in the climate system: A scientific assessment, Journal Of Geophysical
497   Research: Atmospheres, Vol. 118, 5380–5552, doi:10.1002/jgrd.50171, 2013.

498   Braesicke, P., O. J. Smith, P. Telford, and J. A. Pyle.:Ozone concentration changes in the Asian
499   summer monsoon anticyclone and lower stratospheric water vapour: An idealised model
500   study, Geophys. Res. Lett., 38, L03810, doi:10.1029/2010GL046228, 2011.

501   Butt, E. W. Rap A., Schmidt A., Scott C. E., Pringle K. J., Reddington1 C. L., Richards N. A. D.,
502   Woodhouse M. T., Ramirez-Villegas J., Yang H., Vakkari V., Stone E. A., Rupakheti M.,
503   Praveen P. S., van Zyl P. G., Beukes J. P., Josipovic M., Mitchell E. J. S., Sallu S. M.,
504   Forster P. M., and Spracklen D. V.: The impact of residential combustion emissions on
505   atmospheric aerosol, human health, and climate, Atmos. Chem. Phys., 16, 873–905,
506   doi:10.5194/acp-16-873-2016, 2016.

Atmospheric
Chemistry
and Physics
Discussions

509 Carmichael, G. H., Bhupesh Adhikary,Sarika Kulkarni,Alessio D'Allura,Youhua Tang, David
510   Streets,Qiang Zhang,TamI C. Bond, Veerabhadran Ramanathan, Aditsuda Jamroensan,
511   and Pallavi Marrapu, Asian Aerosols: Current and Year 2030 Distributions and
512   Implications to Human Health and Regional Climate Change, Environ. Sci. Technol., 43,
513   5811–5817, doi:10.1021/es8036803, 2009.

514 Cheng, T., Y. Peng, J. Feichter, and I. Tegen.: An Improvement on the dust emission scheme in
515   the global aerosol-climate model ECHAM5-HAM, Atmos. Chem. Phys., 8, 1105-1117,
516   doi:10.5194/acp-8-1105-2008, 2008.

517 Chin, M., Diehl, T., Dubovik, O., Eck, T. F., Holben, B. N., Sinyuk, A., and Streets, D. G.: Light
518   absorption by pollution, dust, and biomass burning aerosols: a global model study and
519   evaluation with AERONET measurements, Ann. Geophys., 27, 3439–3464,
520   doi:10.5194/angeo-27-3439-2009, 2009.

521 Chung, S. H., and J. H. Seinfeld.: Global distribution and climate forcing of carbonaceous
522   aerosols, J. Geophys. Res., 107(D19), 4407, doi:10.1029/2001JD001397, 2002.

523 Das S., Dey S., Dash S. K., Impacts of aerosols on dynamics of Indian summer monsoon using a
524   regional climate model, Clim Dyn., 44:1685–1697, DOI 10.1007/s00382-014-2284-4,
525   2015

526 Deng, M., G. G. Mace, Z. Wang, and H. Okamoto.: Tropical Composition, Cloud and Climate
527   Coupling Experiment validation for cirrus cloud profiling retrieval using CloudSat radar and
528   CALIPSO lidar, J. Geophys. Res., 115, D00J15, doi:10.1029/2009JD013104, 2010.

529 Deng, M., G. G. Mace, Z. Wang, and Lawsan, R. P.: Evaluation of Several A-Train Ice Cloud
530   Retrieval Products with In Situ Measurements Collected during the SPARTICUS Campaign,
531   Journal Of Applied Meteorology And Climatology, 52, 1014-1030, doi: 10.1175/JAMC-D-
532   12-054.1, 2013.

533 Dentener, F., Kinne,S., Bond,T., Boucher,O., Cofala, J., Generoso, S., Ginoux, P., Gong,S.,.
534   Hoelzemann, J., Ito,A., Marelli,L., Penner, J., Putaud, J.P., Textor, C., Schulz, M.,
535   G.V.D., Werf, Wilson J.: Emissions Of primary aerosol and precursor gases in the years
536   2000 and 1750 prescribed data -sets for AeroCom, Atmos. Chem. Phys., 6, 4321-4344,
537   doi:10.5194/acp-6-4321-2006, 2006.

538 Dessler, A. E., and S. C. Sherwood.: Effect of convection on the summertime extratropical lower
539   stratosphere, J. Geophys. Res., 109, D23301, doi:10.1029/2004JD005209, 2004.

Atmospheric
Chemistry
and Physics
Discussions

540 Fadnavis, S., Schultz, M. G., Semeniuk, K., Mahajan, A. S., Pozzoli, L., Sonbawne, S., Ghude,
541   S. D., Kiefer, M., and Eckert, E.: Trends in peroxyacetyl nitrate (PAN) in the upper
542   troposphere and lower stratosphere over southern Asia during the summer monsoon
543   season: regional impacts, Atmos. Chem. Phys., 14, 12725–12743, doi:10.5194/acp-14-
544   12725-2014, 2014.

545 Fadnavis, S., Semeniuk, K., Pozzoli, L., Schultz, M. G., Ghude, S. D., Das, S., and Kakatkar,
546   R.: Transport of aerosols into the UTLS and their impact on the Asian monsoon region
547   as seen in a global model simulation, Atmos. Chem. Phys., 13, 8771–8786,
548   doi:10.5194/acp-13-8771-2013, 2013.

549 Fadnavis, S., Semeniuk, K., Schultz, M. G., Kiefer, M., Mahajan, A., Pozzoli, L., and
550   Sonbawane, S.: Transport pathways of peroxyacetyl nitrate in the upper troposphere and
551   lower stratosphere from different monsoon systems during the summer monsoon season.
552   Atmos. Chem. Phys., 15, 11477-11499, doi:10.5194/acp-15-11477-2015, 2015.

553 Fadnavis, S.; Roy, Chaitri; Sabin, T. P.; Ayantika, D. C.; Ashok, K.: Potential modulations of
554   pre-monsoon aerosols during El Niño: impact on Indian summer monsoon, Clim.Dyn,1-
555   12,doi: 10.1007/s00382-016-3451-6, 2016.

556 Flohn, H.: Large-scale aspects of the summer monsoon in South and East Asia, J. Meteor. Soc.
557   Japan, 75, 180–186, doi: 551.553.21:551.589.5, 1957.

563 Fu, R., Hu, Y., Wright, J. S., Jiang, J. H., Dickinson, R. E., Chen, M., Filipiak, M., Read,W.
564   G.,Waters, J.W., and Wu, D. L.: Short circuit of water vapour and polluted air to the
565   global stratosphere by convective transport over the Tibetan Plateau, P. Natl. Acad. Sci.
566   USA, 103, 5664–5669, doi: 10.1073/pnas.0601584103, 2006.

567 Ganguly, D., P. J. Rasch, H. Wang, and J.-H. Yoon, Climate response of the South Asian
568   monsoon system to anthropogenic aerosols, J. Geophys. Res., 117, D13209,
569   doi:10.1029/2012JD017508, 2012.

570 Garny, H. and Randel, W. J.: Transport pathways from the Asian monsoon anticyclone to the
571   stratosphere, Atmos. Chem. Phys., 16, 2703–2718, doi:10.5194/acp-16-2703-2016,
572   2016.

573 Gautam R., Hsu N. C., Tsay S. C., Lau K. M., Holben B., Bell S., Smirnov A., Li C., Hansell R.,
574   Ji Q., Payra S., Aryal D., Kayastha R., and Kim K. M.: Accumulation of aerosols over the

Atmospheric
Chemistry
and Physics
Discussions

575   Indo-Gangetic plains and southern slopes of the Himalayas: distribution, properties and

576   radiative effects during the 2009 pre-monsoon season, Atmos. Chem. Phys., 11, 12841–

577   12863, doi:10.5194/acp-11-12841-2011, 2011.

578   Gettelman, A., Forster, P., Fujiwara, M., Fu, Q., Vomel, H., Gohar, L. K., Johanson, C., and

579   Ammerman, M.: Radiation balance of the tropical tropopause layer, J. Geophys. Res.,

580   109, D07103, doi:10.1029/2003JD004190, 2004.

581   Goswami, B. N., V. Krishnamurthy, and H. Annamalai, 1999: A broad scale circulation index for

582   the interannual variability of the Indian summer monsoon. Q. J. R. Meteorol. Soc., 125,

583   pp. 611-633, doi: 10.1002/qj.49712555412 1999.

584   Govardhan, G., Satheesh, S.K., Nanjundiah,R., Krishna Moorthy, K., and Babu, S. S.: Possible

585   climatic implications of high altitude emissions of black carbon, Atmos. Chem. Phys.

586   Discuss., doi:10.5194/acp-2017-96, 2017.

587   Guelle, W., Schulz, M., Balkanski,Y., Dentener, F.: Influence of the source formulation on

588   modeling the atmospheric global distribution of sea salt aerosol, J. Geophys. Res., 106,

589   27509-27524, doi:10.1029/2001JD900249, 2001.

590   Guenther, A., Hewitt, C. N., Erickson, D., Fall, R., Geron, C., Graedel, T., Harley, P., Klinger,

591   L., Lerdau, M., Mckay, W. A., Pierce, T., Scholes, B., Steinbrecher, R., Tallamraju, R.,

592   Taylor, J., and Zimmerman, P. A.: Global-Model of Natural Volatile Organic-Compound

593   Emissions, J. Geophys. Res.- Atmos., 100, 8873–8892, **doi:** 10.1029/94JD02950, 1995.

594   Guo L., Highwood E. J., Shaffrey L. C., and Turner A. G.: The effect of regional changes in

595   anthropogenic aerosols on rainfall of the East Asian Summer Monsoon, Atmos. Chem.

596   Phys., 13, 1521-1534, doi:10.5194/acp-13-1521-2013, 2013.

597   Guo, L., Turner. A.G. and Highwood, E. J.: Impacts of 20th century aerosol emissions on the

598   South Asian monsoon in the CMIP5 models, Atmos. Chem. Phys., 15, 6367–6378,

599   doi:10.5194/acp-15-6367-2015, 2015.

600   Guo, L., Turner, A., and Highwood, E. J.: Local and Remote Impacts of Aerosol Species on

601   Indian Summer Monsoon Rainfall in a GCM**,** Journal of Climate, 6937-6955, doi:

602   10.1175/JCLI-D-15-0728.1, 2016.

607   Haywood, J. M., Shine,K.P.: Multi-spectral calculations of the radiative forcing of tropospheric

608   sulphate and soot aerosols using a column model, Q. J. R. Meteorol. Soc., 123, 1907-

609   1930, doi:10.1002/qj.49712354307, 1997.

Atmospheric
Chemistry
and Physics
Discussions

610 He, Q. S., Li, C. C., Ma, J. Z., Wang, H. Q., Yan, X. L., Lu, J., Liang, Z. R., and Qi, G. M.:
611   Lidar-observed enhancement of aerosols in the upper troposphere and lower stratosphere
612   over the Tibetan Plateau induced by the Nabro volcano eruption, Atmos. Chem. Phys.,
613   14, 11687-11696, doi:10.5194/acp-14-11687-2014, 2014.

620 Hirose, M., and K. Nakamura, Spatial and diurnal variation of precipitation systems over Asia
621   observed by the TRMM Precipitation Radar, J. Geophys. Res., 110, D05106,
622   doi:10.1029/2004JD004815, 2005.

623 Hodnebrog, O., Myhre,G., Samset, B.H .: How shorter black carbon lifetime alters its climate
624   effect, Nature Communications, 5, doi:10.1038/ncomms6065, 2014.

625 Horowitz, L. W., Walters, S., Mauzerall, D. L., Emmons, L. K., Rach, P. J., Granier, C., Tie, X.,
626   Lamarque, J., Schultz, M.G.,Tyndall, G. S., Orlando, J. J., and Brasseur, G. P.: A global
627   simulation of tropospheric ozone and related tracers: Descriptionand evaluation of
628   MOZART, version 2, J. Geophys. Res., 108, 4784, doi:10.1029/2002JD002853, 2003.

629 Huffman, G.J., R.F. Adler, D.T. Bolvin, G. Gu, E.J. Nelkin, K.P. Bowman, Y. Hong, E.F.
630   Stocker, D.B. Wolff.: The TRMM Multi-satellite Precipitation Analysis: Quasi-Global,
631   Multi-Year, Combined-Sensor Precipitation Estimates at Fine Scale. J.
632   Hydrometeor., 8(1) ,38-55,doi: http://dx.doi.org/10.1175/jhm560.1, 2007.

633 Jacobson, M. C., Hansson, H.-C., Noone, K. J., and Charlson, R. J.: Organic atmospheric
634   aerosols: Review and state of the science, Rev. Geophys., 38, 267–294,
635   doi: 10.1029/1998RG000045, 2000.

636 Kang, I.S., Jin, K., Wang, B., Lau, K.M., Shukla, J., Krishnamurthy, V., Schubert,S., Waliser,
637   D., Stern,W., Kitoh,A., Meehl,G., Kanamistu,M., Galin,V., Satyan,V., Park,C.K.,Liu,Y.:
638   Intercomparison of the climatological variations of Asian summer monsoon precipitation
639   simulated by 10 GCMs, Clim. Dyn, 19: 383–395, doi:10.1007/s00382-002-0245-9, 2002.

640 Kloster, S., Dentener, F., Feichter, J., Raes, F., Lohmann, U., Roeckner, E., Burns,I.F.: A GCM
641   study of future climate response to aerosol pollution reductions, Clim. Dyn,
642   doi:10.1007/s00382-009-0573-0, 2009.

643 Kopp, R. E., Mauzeralla D. L.: Assessing the climatic benefits of black carbon mitigation,
644   PNAS, 107, 26, 11703-11708, doi: 10.1073/pnas.0909605107, 2010.

645 Krishnamurthy V, Achuthavarier D.: Intraseasonal oscillations of the monsoon circulation over
646   South Asia. Clim. Dyn, 38(11):2335–2353, doi: 10.1007/s00382-011-1153-7, 2012.

Atmospheric
Chemistry
and Physics
Discussions

Open Access

647 Kumar, R., Naja, M., Satheesh, S.K., Ojha, N., Joshi, H., Sarangi, T., Pant, P., Dumka, U.C.,
648   Hegde, P., Venkataramani, S.: Influences of the springtime northern Indian biomass
649   burning over the central Himalayas, J. Geophys. Res., 116, D19302,
650   doi:10.1029/2010JD015509, 2011.

651 Kummerow, C., Barnes, W., Kozu, T., Shiue, J. and Simpson, J.: The Tropical Rainfall
652   Measuring Mission (TRMM) sensor package. J. Atmos. Oceanic Technol., 15, 809–816,
653   doi: http://dx.doi.org/10.1175/1520-0426(1998)015<0809:TTRMMT>2.0.CO;2, 1998.

654 Kunze M., Braesicke P., Langematz U., Stiller G., Bekki S, Brühl C., Chipperfield M., Dameris
655   M., Garcia R, and Giorgetta M.: Influences of the Indian Summer Monsoon on Water
656   Vapor and Ozone Concentrations in the UTLS as Simulated by Chemistry–Climate
657   Models, 23, 3525-3544, do1: 10.1175/2010JCLI3280, 2010.

658 Lamarque, J.F., Bond, T.C., Eyring,V., Granier, C., Heil,A., Klimont, A., Lee, D., Liousse,D.,
659   Mieville, A., Owen,B., Schultz, M.G., Shindell, D., Smith, S.J., Stehfest,E., Van
660   Aardenne,J., Cooper4,O.R., Kainuma, M., Mahowald, N., JMcConnell, J.R., Naik,V.,
661   Riahi, K., van Vuuren, D.P .: Historical (1850–2000) gridded anthropogenic and biomass
662   burning emissions of reactive gases and aerosols: methodology and application, Atmos.
663   Chem. Phys., 10, 7017- 7039, doi:10.5194/acp-10-7017-2010, 2010.

664 Lau, K. M., Kim, K. M.: Observational relationships between aerosol and Asian monsoon
665   rainfall, and circulation, Geophys. Res. Lett., 33, L21810, doi:10.1029/2006GL027546,
666   2006.

667 Lelieveld, J., Crutzen, P. J., Ramanathan, V., Andreae, M. O., Brenninkmeijer, C. A. M.,
668   Campos, T., Cass, G. R., Dickerson, R. R., Fischer, H., de Gouw, J. A., Hansel, A.,
669   Jefferson, A., Kley, D., de Laat, A. T. J., Lal, S., Lawrence, M. G., Lobert, J. M., Mayol-
670   Bracero, O. L., Mitra, A. P., Novakov, T., Oltmans, S. J., Prather, K. A., Reiner, T.,
671   Rodhe, H., Scheeren, H. A., Sikka, D., and Williams, J.: The Indian Ocean Experiment:
672   Widespread Air Pollution from South and Southeast Asia, Science, 291, 1031– 1036, ,
673   doi: 10.1126/science.1057103, 2001.

674   Li, C. and Yanai M.: The onset and interannual variability of the Asian summer monsoon in
675   relation to land–sea thermal contrast, J. Clim. 9: 358–375, doi:
676   http://dx.doi.org/10.1175/1520-0442(1996)009,0358:TOAIVO>2.0.CO;2, 1996.

Atmospheric
Chemistry
and Physics
Discussions

677 Li, J.-L. F., Walilser, D.E., Chen. W.T., Guan, B., Kubar, T., Stephens, G., Ma, H.Y., Deng, M.,
678   Donner, L., SEman, C., Horowitz, L.: An observationally based evaluation of cloud ice
679   water in CMIP3 and CMIP5 GCMs and contemporary reanalyses using contemporary
680   satellite data, J. Geophys. Res., 117, D16105, doi:10.1029/2012JD017640, 2012.

681 Li, J.-L. F., Waliser, D. E., Stephens, G., Lee, S., L'Ecuyer, T., Kato, S., Loeb, N. and Ma, H.
682   Y.: Characterizing and understanding radiation budget biases in CMIP3/CMIP5 GCMs,
683   contemporary GCM, and reanalysis. J. Geophys. Res., 118, 8166–8184,
684   doi:10.1002/jgrd.50378, 2013.

685 Li, Q., Jiang, J. H., Wu, D. L., Read, W. G., Livesey, N. J.,. Waters, J.W:, Zhang, Y.,Wang, B.,
686   Filipiak, M. J., Davis, C. P., Turquety,S., Wu, S., Park R. J., Yantosca R. M., and Jacob
687   D. J.: Convective outflow of South Asian pollution: A global CTM simulation compared
688   with   EOS   MLS   observations,   Geophys.   Res.   Lett.,   32,   L14826,
689   doi:10.1029/2005GL022762, 2005.

690 Lin C-Y, Zhao C., Liu X., Lin N-H ., ChenW-N.: Modelling of long-range transport of southeast
691   Asia biomass-burning aerosols to Taiwan and their radiative forcings over EAST
692   ASIA,Tellus B 2014, 66, 23733, http://dx.doi.org/10.3402/tellusb.v66.23733, 2014.

693 Lin N. H., Tsay, Si-C., Maring, H.B., Yen, M.Ch., Sheu,G.R., Wang, S.H., Chi, K.H., Chuang,
694   M.T., Chang-Feng Ou-Yang , Joshua S. Fu, Jeffrey S. Reid, Chung-Te Lee, Lin-Chi
695   Wang, Jia-Lin Wang , Christina N. Hsu , Andrew M. Sayer, Brent N. Holben, Yu-Chi
696   Chu, Xuan Anh Nguyen, Khajornsak Sopajaree , Shui-Jen Chen, Man-Ting Cheng, Ben-
697   Jei Tsuang, Chuen-Jinn Tsai, Chi-Ming Peng, Russell C. Schnell, Tom Conway, Chang-
698   Tang Chang , Kuen-Song Lin, Ying I. Tsai, Wen-Jhy Lee, Shuenn-Chin Chang, Jyh-Jian
699   Liu, Wei-Li Chiang, Shih-Jen Huang, Tang-Huang Lin, Gin-Rong Liu.: An overview of
700   regional experiments on biomass burning aerosols and related pollutants in Southeast
701   Asia: From BASE-ASIA and the Dongsha Experiment to 7-SEAS, Atmos. Environ., 78,
702   1-19, http://dx.doi.org/10.1016/j.atmosenv.2013.04.066, 2013.

703 Liu, H.-L., Wang, P.K., Schlesinger, R.E.: A numerical study of cirrus clouds. Part II: Effects of
704   Ambient Temperature, Stability, Radiation, Ice Microphysics, and Microdynamics on
705   Cirrus Evolution. J. Atmos. Sci. 60, 1097–1119, doi: http://dx.doi.org/10.1175/1520-
706   0469(2003)060<1097:ansocc>2.0.co;2, 2003.

Atmospheric
Chemistry
and Physics
Discussions

Open Access

707   Lohmann U., Ferrachat, S.: Impact of parametric uncertainties on the present-day climate and on
708   the anthropogenic aerosol effect, Atmos. Chem. Phys., 10, 11373-11383,
709   doi:10.5194/acp-10-11373-2010, 2010.

710   Lu, Z., Zhang, Q., Streets, D. G.: Sulfur dioxide and primary carbonaceous aerosol emissions in
711   China and India, 1996–2010, Atmos. Chem. Phys., 11, 9839–9864, doi:10.5194/acp-11-
712   9839- 2011, 2011.

713   Manoj M. G., Devara, P.C.S., Safai, P.D., Goswami, B.N.: Absorbing aerosols facilitate
714   transition of Indian monsoon breaks to active spells, Clim. Dyn, 37:2181–2198, doi:
715   10.1007/s00382-010-0971-3, 2011.

716   Mao, Y. H., Li, Q. B., Chen, D., Zhang, L., Hao, W.-M., and Liou, K.-N.: Top-down estimates of
717   biomass burning emissions of black carbon in the Western United States, Atmos. Chem.
718   Phys., 14, 7195–7211, doi:10.5194/acp-14-7195-2014, 2014.

719   Meehl G A, Arblaster J.M., Collins, W.D.: Effects of black carbon aerosols on the Indian
720   monsoon, J. Climate, 21, 2869–2882, doi: http://dx.doi.org/10.1175/2007JCLI1777.1,
721   2008.

722   Meehl, G. A.: Coupled land-ocean-atmosphere processes and South Asian monsoon variability,
723   Science, 266, 263–267, doi: 10.1126/science.266.5183.263, 1994.

724   Menon, S., Hansen, J., Nazarenko, L., and Luo, Y.: Climate Effects of Black Carbon Aerosols in
725   China and India, Science, 297, 2250–2253, doi: 10.1126/science.1075159, 2002.

726   Mieville, A., C. Granier, C. Liousse, B. Guillaume, F. Mouillot, J.F. Lamarque, J.M. Gregoire,
727   and G. Petron.: Emissions of gases and particles from biomass burning using satellite
728   data   and   an   historical   reconstruction,   Atmos.   Environ.,   44,   1469–1477,
729   doi:10.1016/j.atmosenv.2010.01.011, 2010.

730   Myhre, G., D. Shindell, F.-M. Bréon, W. Collins, J. Fuglestvedt, J. Huang, D. Koch, J.-F.
731   Lamarque, D. Lee, B. Mendoza, T. Nakajima, A. Robock, G. Stephens, T. Takemura and
732   H. Zhang, Anthropogenic and Natural Radiative Forcing. In: Climate Change 2013: The
733   Physical Science Basis. Contribution of Working Group I to the Fifth Assessment Report
734   of the Intergovernmental Panel on Climate Change [Stocker, T.F., D. Qin, G.-K. Plattner,
735   M. Tignor, S.K. Allen, J. Boschung, A. Nauels, Y. Xia, V. Bex and P.M. Midgley (eds.)].
736   Cambridge University Press, Cambridge, United Kingdom and New York, NY, USA.,
737   2013.

738 Neubauer D., Lohmann U. and Hoose C. and Frontoso, M. G.: Impact of the representation of
739 marine stratocumulus clouds on the anthropogenic aerosol effect Atmos. Chem. Phys.,
740 14, 11997–12022, doi:10.5194/acp-14-11997-2014, 2014.
741 Park, M., Randel, W. J., Emmons, L. K., Livesey, N. J.: Transport pathways of carbon monoxide
742 in the Asian summer monsoon diagnosed from Model of Ozone and Related Tracers
743 (MOZART), J. Geophys. Res., 114, D08303, doi:10.1029/2008JD010621, 2009.
744 Park, M., Randel, W.J., Emmons, L.K., Bernath, P.F., Walker, K.A., Boone, C.D.: Chemical
745 isolation in the Asian monsoon anticyclone observed in Atmospheric Chemistry
746 Experiment (ACE-FTS) data, Atmos. Chem. Phys., doi:10.5194/acp-8-757-2008,2008.
747 Park, M., Randel,W.J., Gettelman, A., Massie, S.T., Jiang, J.H.:Transport above the Asian
748 summer monsoon anticyclone inferred from Aura Microwave Limb Sounder tracers, J.
749 Geophys. Res., 112, D16309, doi:10.1029/2006JD008294, 2007.
750 Penner, J. E., Chuang, C.C., Grant, K.: Climate forcing by carbonaceous and sulfate aerosols,
751 Clim. Dyn., 14, 839 -851, doi:10.1007/s003820050259, 1998.
752 Ploeger F., Konopka P., Müller R., Fueglistaler S., Schmidt T., Manners J., Grooss J.-U.,
753 Günther G., de Forster P.M., and Riese M., Horizontal transport affecting trace gas
754 seasonality in the tropical tropopause layer TTL, J. Geophys. Res., 117,
755 D09303,doi:10.1029/2011JD017267, 2012.
756 Ploeger, F., Fueglistaler, S., Grooß, J.-U., Günther, G., Konopka, P., Liu, Y. S., Müller, R.,
757 Ravegnani, F., Schiller, C., Ulanovski, A., and Riese, M.: Insight from ozone and water
758 vapour on transport in the tropical tropopause layer (TTL), Atmos. Chem. Phys., 11, 407-
759 419, doi:10.5194/acp-11- 407-2011, 2011.
760 Ploeger, F., G. Günther, P. Konopka, S. Fueglistaler, R. Müller, C. Hoppe, A. Kunz, R. Spang,
761 J.-U. Grooß, and M.Riese , Horizontal water vapor transport in the lower stratosphere
762 from subtropics to high latitudes during boreal summer, J. Geophys. Res. Atmos., 118,
763 8111–8127, doi:10.1002/jgrd.50636, 2013.
764 Powell K., Vaughan M., Winker D.,K. M. Lee, Pitts M., Trepte C.: CALIPSO Data Product
765 Catalog,Release 3.6, Document No: PC-SCI-503, 2013.
766 Ramanathan, V., Crutzen, P. J., Lelieveld, J., Mitra, A. P., Althausen,D., Anderson, J., Andreae,
767 M. O., Cantrell, W., Cass,G. R., Chung, C. E., Clarke, A. D., Coakley, J. A., Collins,W.
768 D.,Conant, W. C., Dulac, F., Heintzenberg, J., Heymsfield, A. J.,Holben, B., Howell, S.,

Atmospheric
Chemistry
and Physics
Discussions

769   Hudson, J., Jayaraman, A., Kiehl, J. T.,Krishnamurti, T. N., Lubin, D., McFarquhar, G.,

770   Novakov, T.,Ogren, J. A., Podgorny, I. A., Prather, K., Priestley, K., Prospero,J. M.,

771   Quinn, P. K., Rajeev, K., Rasch, P., Rupert, S., Sadourny,R., Satheesh, S. K., Shaw, G.

772   E., Sheridan, P., and Valero, F. P. J.: Indian Ocean Experiment: An integrated analysis of

773   the climateforcing and effects of the great Indio-Asian haze, J. Geophys.Res., 106,

774   28371–28398, 2001a.

775   Ramanathan, V., Crutzen, P. J., Kiehl, J. T. and Rosenfeld, D., Aerosols, Climate, and the

776   Hydrological Cycle , Science 294, 2119–2124, doi: 10.1126/science.1064034, 2001b.

777   Ramanathan V. Crutzen P. J.: New directions: Atmospheric brown "clouds", Atmos.

778   Environ. 37:4033–4035, doi:10.1016/S1352-2310(03)00536-3, 2003.

779   Ramanathan, V. and Carmichael, G.: Global and regional climate changes due to black carbon,

780   Nat. Geosci., 1, 221–227, doi:10.1038/ngeo156, 2008.

781   Ramaswamy, V., Ramanathan, V. Solar absorption of cirrus clouds and the maintenance of the

782   tropical upper troposphere thermal structure. J. Atmos. Sci. 46, 2293–2310, doi:

783   http://dx.doi.org/10.1175/1520-0469(1989)046<2293:SABCCA>2.0.CO;2 1989.

784   Randall, D.A., Harshovardan, Dazlich, D.A., Corsetti, T.G. Interactions among radiation,

785   convection, and large-scale dynamics in a general circulation model. J. Atmos. Sci. 46,

786   1943–1970, doi:10.1175/1520-0469(1989)046<1943:IARCAL>2.0.CO;2, 1989.

787   Randel, W. J., Park, M., Emmons, L., Kinnison, D., Bernath, P., Walker, K. A., Boone, C., and

788   Pumphrey H.: Asian monsoon transport of pollution to the stratosphere, Science, 328,

789   611–613, doi: 10.1126/science.1182274, 2010.

790   Randel,W. J. and Park, M.: Deep convective influence on the Asian summer monsoon

791   anticyclone and associated tracer variability observed with Atmospheric Infrared Sounder

792   (AIRS), J. Geophys. Res., 111, D12314, doi:10.1029/2005JD006490, 2006.

793   Rosenfield, D., Suppression of rain and snow by urban and industrial air pollution, Science, 287,

794   1793–1796, doi: 10.1126/science.287.5459.1793, 2000.

795   Satheesh, S. K. and Ramanathan, V.: Large differences in tropical aerosol forcing at the top of

796   the atmosphere and Earth's surface, Nature, 405, 60–63, doi:10.1038/35011039, 2000.

797   Schultz, M. G., Heil, A., Hoelzemann, J. J., Spessa, A., Thonicke, K., Goldammer, J., Held, A.

798   C., Pereira, J. M., and van het Bolscher, M.: Global wildland fire emissions from 1960 to

799   2000, Global Biogeochem. Cyc., 22, GB2002, doi:10.1029/2007GB003031,2008.

800 Solomon, S., D. Qin, M. Manning, Z. Chen, M. Marquis, K.B. Averyt, M. Tignor and H.L.
801   Miller, Contribution of Working Group I to the Fourth Assessment Report of the
802   Intergovernmental Panel on Climate Change,Cambridge University Press, Cambridge,
803   United Kingdom and New York, NY, USA. 2007.

804 Stephens, G. L., Vane, D.G., Taneeli, S., Im,E., Durden, S., Rockey, M., Reinke, D., Partain, P.,
805   Mace, G.G., Austin, R., Ecuyet, T.L., Haynes, J., Lebsock, M., Suzuki, K., Waliser, D.,
806   Wu, D., Kay, J., Gettelman, A., Wang, Z., Marchand, R.: CloudSat mission: Performance
807   and early science after the first year of operation, J. Geophys. Res., 113, D00A18,
808   doi:10.1029/2008JD009982, 2008.

809 Stevens, B., Giorgetta M., Esch M., Mauritsen T., Crueger T., Rast S., Salzmann M., Schmidt H.,
810   Bader J., Block K., Brokopf R., Fast I., Kinne S., Kornblueh L., Lohmann U., Pincus R.,
811   Reichler T., and Roeckne E., Atmospheric component of the MPI-M Earth System
812   Model: ECHAM6, J. of Advances in Modeling Earth Systems. **5**, 1–27,
813   doi:10.1002/jame.20015, 2013.

814 Stier, P., J. Feichter, S. Kinne, S. Kloster, E. Vignati, J. Wilson, L. Ganzeveld, I. Tegen, M.
815   Werner, Y. Balkanski, M. Schulz, O. Boucher, A. Minikin, and A. Petzold, 2005.:The
816   aerosol-climate model ECHAM5-HAM, Atmos. Chem. Phys., **5**, 1125-1156,
817   doi:10.5194/acp-5-1125-2005, 2005.

818 Streets, D. G., Yan, F., Chin, M., Diehl, T., Mahowald, N., Schultz, M., Wild, M., Wu, Y., and
819   Yu, C.: Anthropogenic and natural contributions to regional trends in aerosol optical
820   depth, 1980–2006, J. Geophys. Res., 114, D00D18, doi:10.1029/2008jd011624, 2009.

821 Takahashi, H. G.: Seasonal and diurnal variations in rainfall characteristics over the tropical
822   Asian monsoon region using TRMM-PR data. SOLA, 12A, 22−27, doi:10.2151/
823   sola.12A-005, 2016.

824 Tegen, I., Harrison, S. P., Kohfeld, K., Prentice, I. C., Coe, M., and Heimann, M.: Impact of
825   vegetation and preferential source areas on global dust aerosol: Results from a model
826   study, J. Geophys. Res.-Atmos., 107, 4576, doi:10.1029/2001JD000963, 2002.

827 Thomason, L. W. and Vernier, J.P.: Improved SAGE II cloud/aerosol categorization and
828   observations of the Asian tropopause aerosol layer: 1989–2005, Atmos. Chem. Phys., 13,
829   4605-4616, doi:10.5194/acp-13-4605-2013, 2013.

Atmospheric
Chemistry
and Physics
Discussions

830   Tobo, Y., Iwasaka, Y., Yu Shi, G.,Kim, Y. S., Ohashi, T, Tamura, K. and Zhang, D.: Balloon-
831   borne observations of high aerosol concentrations near the summertime tropopause
832   over the Tibetan Plateau, Atmospheric Research, 84, 233–241,
833   doi:10.1016/j.atmosres.2006.08.003, 2007.

839   Tripathi, S.N., Srivastava, A.K., S. Dey, S., Satheesh, S.K., Krishnamoorthy,K.: The vertical
840   profile of atmospheric heating rate of black carbon aerosols at Kanpur in northern India,
841   Atmos. Environ., 41,6909–6915, doi: http://dx.doi.org/10.1016/j.atmosenv.2007.06.032,
842   2007.

846   Van derWerf, G. R., Randerson, J.T., Giglio, L., Collatz, G.J., Kasibhatla, P.S., Arellano A.F.:
847   Interannual variability in global biomass burning emissions from 1997 to 2004, Atmos.
848   Chem. Phys., **6**, 3423-3441, doi:10.5194/acp-6-3423-2006, 2006.

849   Vernier, J. P., L. W. Thomason, and J. Kar.: CALIPSO detection of an Asian tropopause aerosol
850   layer, Geophys. Res. Lett., 38, L07804, doi:10.1029/2010GL046614, 2011.

851   Vernier, J.P., Fairlie, T.D., Natarajan, M., Wienhold, F.G., Bian, J., Martinsson, B.G.,
852   Crumeyrolle, S., Thomason, L.W., Bedka, K.M.: Increase in upper tropospheric and
853   lower stratospheric aerosol levels and its potential connection with Asian pollution, J.
854   Geophys. Res. Atmos., 120, 1608–1619, doi:10.1002/2014JD022372, 2015.

855   Vignati, E., Wilson,J., and Stier,P.: An efficient size-resolved aerosol microphysics module for
856   large-scale aerosol transport models, J. Geophys. Res., 109, D22202,
857   doi:10.1029/2003JD004485, 2004.

858   Vogel B., Günther G., Müller R., Grooß J.-U., and Riese M., Impact of different Asian source
859   regions on the composition of the Asian monsoon anticyclone and of the extratropical
860   lowermost stratosphere, Atmos. Chem. Phys., 15, 13699–13716, doi:10.5194/acp-15-
861   13699-2015, 2015.

862   Vogel B., Pan L. L., Konopka P., Günther G., Müller R., Hall W., Campos T., Pollack T.,
863   Weinheimer A., Wei J., Atlas E. L. and Bowman K.P., Transport pathways and
864   signatures of mixing in the extratropical tropopause region derived from Lagrangian
865   model simulations, J. Geophys. Res., 116, D05306, doi:10.1029/2010JD014876, 2011.

866   Wang, B. and Linho, Rainy Season of the Asian–Pacific Summer Monsoon, Journal of Climate,
867   15, 386-398, http://dx.doi.org/10.1175/1520-0442(2002)015<0386:RSOTAP>2.0.CO;2
868   2002.

Atmospheric
Chemistry
and Physics
Discussions

869   Wang, C. A modeling study on the climate impacts of black carbon aerosols, J. Geophys. Res.,
870   109, D03106, doi:10.1029/2003JD004084, 2004.

871   Wang, C., Impact of direct radiative forcing of black carbon aerosols on tropical convective
872   precipitation, Geophys. Res. Lett., 34, L05709, doi:10.1029/2006GL028416, 2007.

873   Wang, C., Kim, D., Ekman, A. M. L.,. Barth, M. C and Rasch, P. J.: Impact of anthropogenic
874   aerosols   on   Indian   summer   monsoon,   Geophys.   Res.   Lett.,   36,   L21704,
875   doi:10.1029/2009GL040114, 2009.

876   Winiger P., Andersson A., Eckhardt S., Stohl A. and Gustafsson O.:The sources of atmospheric
877   black carbon at a European gateway to the Arctic, Nature Communications, 7, 12776,
878   doi: 10.1038/ncomms12776, 2016.

879   Winker D, Pelon J, Coakley J, Ackerman S, Charlson R, Colarco P, Flamant P, Fu Q, Hoff R,
880   Kittaka C, Kubar, T.L, Le Treut, H., McCormick, M.P., Mégie,G., Poole,L., Powell, K.,
881   Trepte, C., Vaughan, M.A., Wielicki, B.A.:THE CALIPSO MISSION A Global 3D View
882   of   Aerosols   and   Clouds.   Bull   Amer   Meteorol   Soc.,   91,   1211-1229,   doi:
883   http://dx.doi.org/10.1175/2010bams3009.1, 2010.

884   Wu G, Zhang Y. : Tibetan Plateau forcing and timing of the monsoon onset over South Asia and
885   South   China   Sea,   Monthly   Weather   Review,   126,   913–927,   doi:
886   http://dx.doi.org/10.1175/1520-0493(1998)126<0913:tpfatt>2.0.co;2, 1998

887   Xie, P., Yatagai,A., Chen, M., Hayasaka, T., Fukushima, Y., Liu, C., Yang, S.: A Gauge-
888   Based Analysis of Daily Precipitation over East Asia, Journal of Hydrometeorology, doi:
889   10.1175/JHM583.1, 2007.

890   Xiong, X., Houweling, S., Wei, J., Maddy, E., Sun, F., and Barnet, C.: Methane plume over
891   south Asia during the monsoon season: satellite observation and model simulation,
892   Atmos. Chem. Phys., 9, 783–794, doi:10.5194/acp-9-783-2009, 2009.

893   Yanai, M., Li, C., Song, Z.: Seasonal heating of the Tibetan Plateau and its effects on the
894   evolution of the Asian summer monsoon, J Meteor Soc Japan, 70, 189–221, 1992.

895   Yu, P., Toon, O.B., Neely, R.R., Martinsson, B.G., Brenninkmeijer, C.A.M.: Composition and
896   physical properties of the Asian Tropopause Aerosol Layer and the North American
897   Tropospheric Aerosol Layer, Geophys. Res. Lett., 42, 2540–2546, doi:10.1002/, 2015.

898   Zhang K., D. O'Donnell, J. Kazil, P. Stier, S. Kinne, U. Lohmann, S. Ferrachat, B. Croft, J.
899   Quaas, H, Wan, S. Rast, and J. Feichter 2012.: The global aerosol-climate model

900 ECHAM-HAM, Version 2: Sensitivity to improvements in process representations,

901 Atmos. Chem. Phys., **12**, 8911-8949, doi:10.5194/acp-12-8911-2012, 2012.

902 Zhang L., Henze D. K., Grell G. A., Carmichael G. R., Bousserez N., Zhang Q., Torres O., Ahn

903 C., Lu Z., Cao J., and Mao Y.: Constraining black carbon aerosol over Asia using OMI

904 aerosol absorption optical depth and the adjoint of GEOS-Chem, Atmos. Chem. Phys.,

905 15, 10281–10308, doi:10.5194/acp-15-10281-2015, 2015.

906 Zveryaev I.I. and. Aleksandrova Marina P.: Differences In Rainfall Variability In The South And

907 Southeast Asian Summer Monsoons, Int. J. Climatol. **24**: 1091–1107, doi:

908 10.1002/joc.1044, 2004.

909

Atmospheric
Chemistry
and Physics
Discussions

Open Access

EGU

910   Table-1: ECHAM6 HAM simulated total (shortwave and long wave together) radiative forcing

911   (W/m^2) and averaged over ASM region

Model Run	TOA	Surface	Atmosphere
DEMISS	-4.2	-12.1	7.9
CTRL	-5.4	-10.6	5.2
Anomalies	1.2	-1.4	2.7

912
913
914
915
916

917
918
919
920
921
922
923
924
925
926
927
928
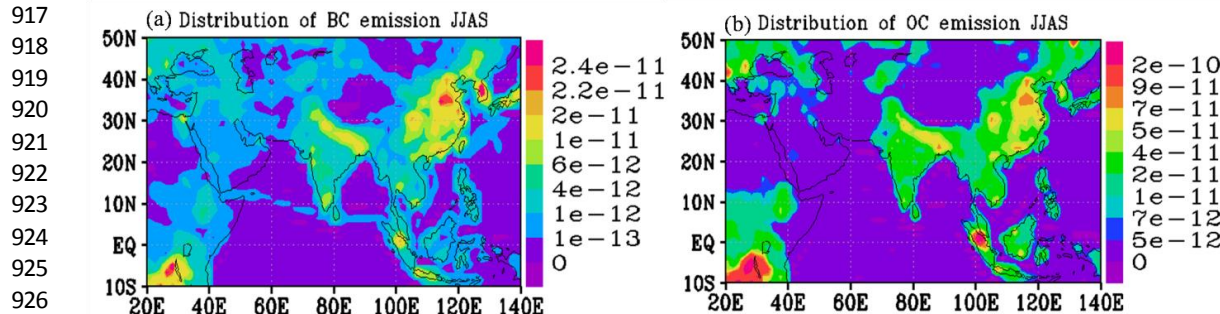
929 Figure1: Distribution of emission mass flux (kg m^{-2} s^{-1}) averaged for the monsoon season (June-
930 September) for **(a)** BC and **(b)** OC aerosols.

931
932
933
934
935
936
937
938
939
940
941
942
943
944
945
946
947
948
949
950
951
952
953
954
955
956
957
958

959

960
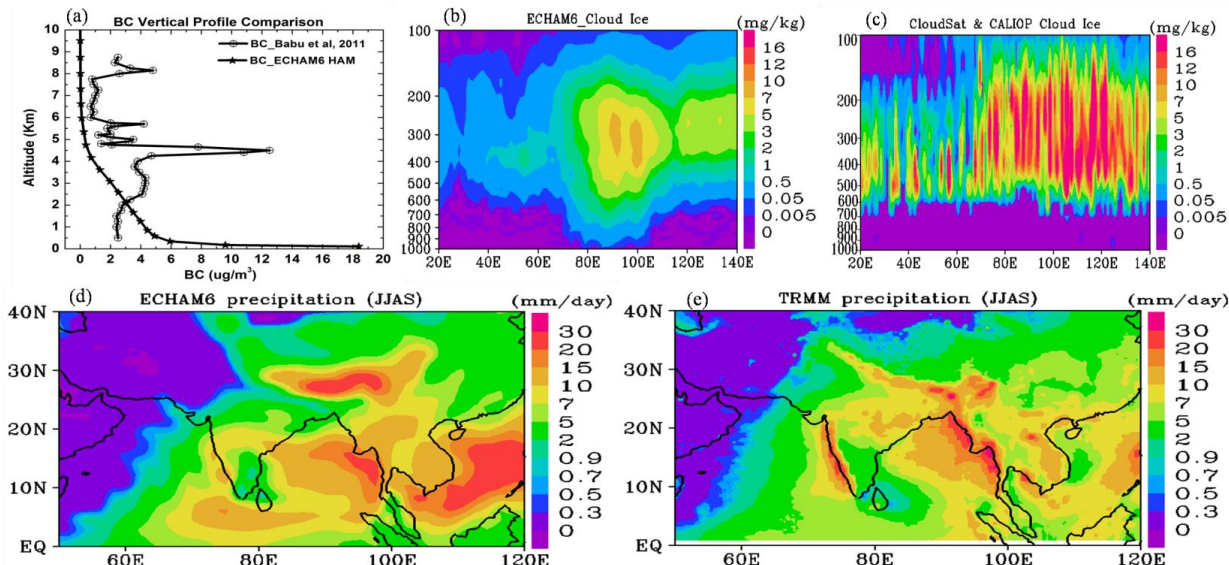
Figure 2: (a) Vertical distribution of BC aerosols (μg/m^3) measurements on 17 March 2010 at Hyderabad (17.48 °N,78.40° E) , India (Babu et al., 2011) and ECHAM6-HAM simulated BC aerosols from CTRL simulations avegraed for month of March at a grid centred at 17°N and 78°E, Longitude-pressure distribution of cloud ice mass mixing ratio (mg/kg) averaged for the monsoon season and 20-40°N (b) ECHAM6-HAM CTRL simulation (c) CloudSat and CALIPSO combined 2C-ICE L3 for the years 2007-2010, (d) seasonal mean precipitation (mm/ day) obtained from (d) ECHAM6-HAM CTRL simulation (e) TRMM averaged for period 1998-2005.

969

970

Atmospheric
Chemistry
and Physics
Discussions
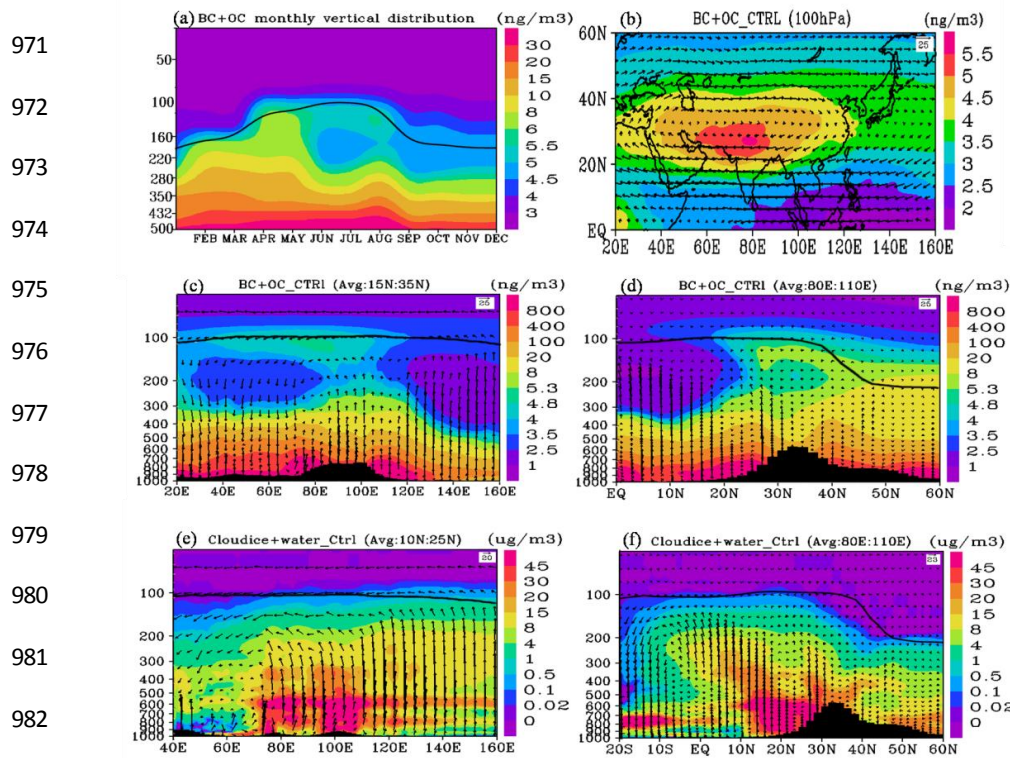
Figure 3: Distribution of BC and OC aerosols (ng/m^3) together (a) monthly variations averaged for the region 70°E - 120°E, 25°E - 45°E, (b) averaged for the monsoon season and at 100 hPa, (c) longitude-presure cross section averaged for 15°N - 35°N and monsoon season (d) latitude-pressure cross section averaged for 80°E - 110°E and monsoon season, Distribution of cloud ice+cloud water (μg m^3) (e) longitude-presure cross section averaged for 10°N - 25°N and monsoon season (f) latitude-pressure cross section averaged for 80°E - 110°E and monsoon season. Black arrows indicate wind vectors. The vertical velocity field has been scaled by 1000. The black line represents the tropopause. In Figs. (a), (c), (d), (e), (f) tropopause is averaged over the same region where field parameter is averaged.
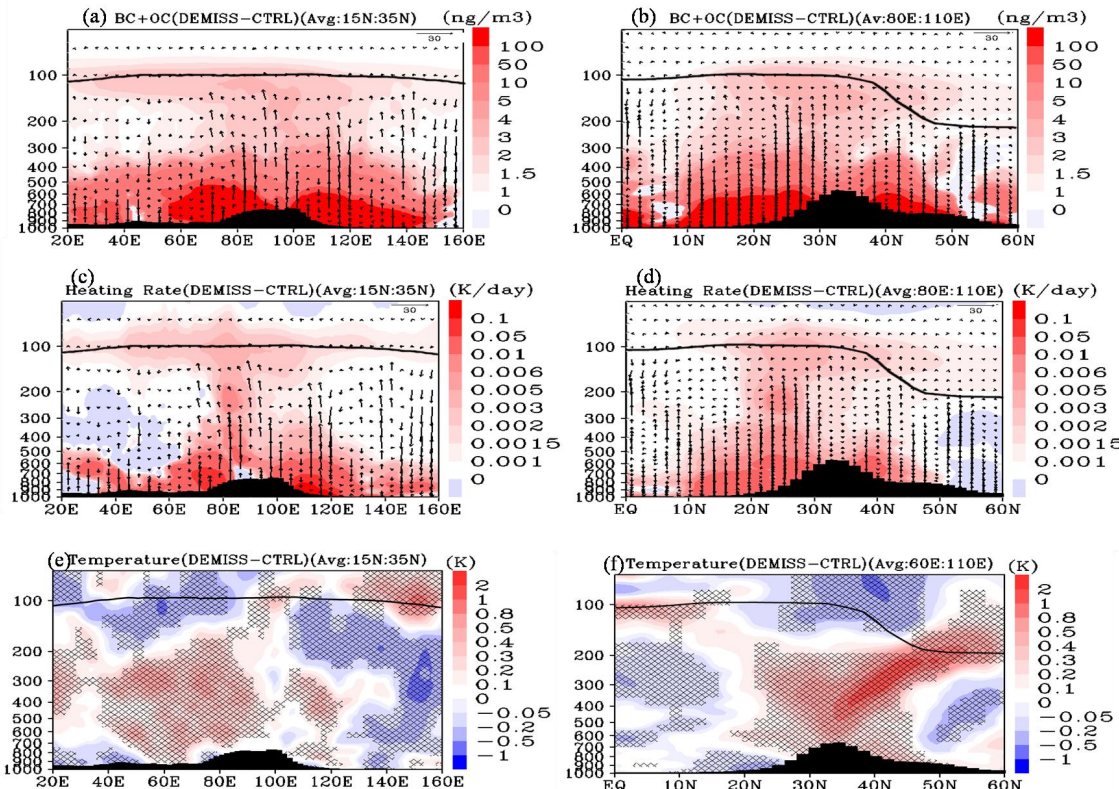
994

995

996   Figure 4: Distribution of anomalies (DEMISS - CRTL), of BC and OC aerosols (ng/m^3) together

997   averaged for the monsoon season (a) longitude-pressure cross section (averaged over 15°N -

998   35°N) (b) latitude-pressure crosssection (averaged over 80°E-110°E), (c) and (d) same as (a) and

999   (b) but for heating rate anomalies (K/day), Black arrows indicate wind vectors (the vertical

1000 velocity field has been scaled by 1000). Distribution of anomalies in temperature (K) (e)

1001 longitude-pressure cross section (averaged over 15°N-35°N), (f) latitude-pressure cross section

1002 (averaged over 60°E -110°E). In Figs (e) and (f) black hatched lines indicate 99% confidence

1003 level. The black line represents the tropopause. The tropopause is averaged over15°N -35°N for

1004 Figs. (a), (c) , (e) and over 80°E-110°E for Figs. (b), (d) and (f).

1005

1006
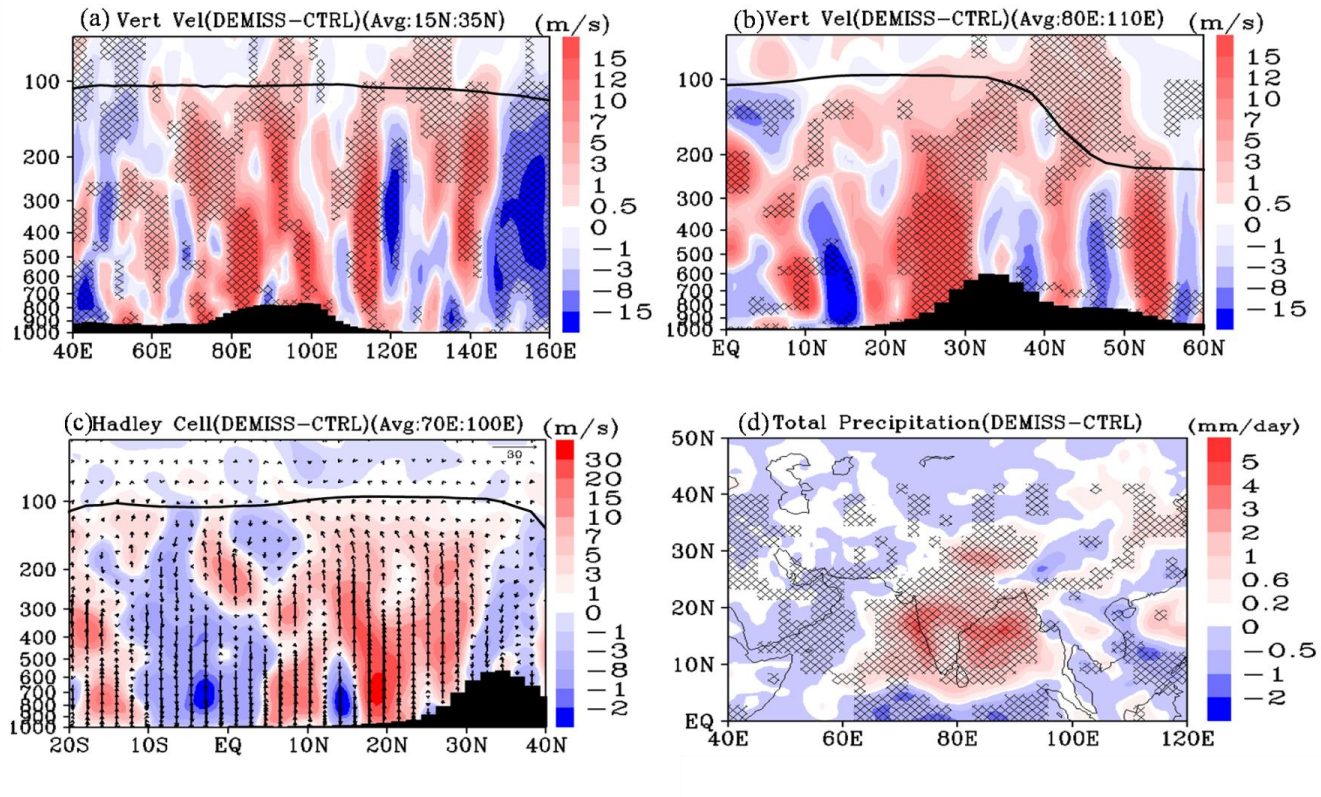
Figure 5: Distribution of anomalies in vertical velocities (m s^{-1}) (DEMISS – CRTL) averaged for the monsoon season (a) longitude-pressure (ageraged over 15ºN - 35ºN) (b) latitude-pressure distribution of (averaged over 80ºE-110ºE), (c) Difference in the meridional circulation due to enhanced carbonaceous aerosols emissions averaged for the monsoon season and over 70ºE-100ºE. Black arrows indicate wind vectors. In Figs (a)-(c) the vertical velocity field has been scaled by 1000 and the thick black line shows the tropopause. The tropopause is averaged over 15°N -35°N for Figs. (a), (c) and over 80ºE-110ºE for Fig. (b), (d) distribution of anomalies of total precipitation (mm/day) averaged for the monsoon season. In Figs (a), (b) and (d) hatched lines indicate 99% confidence level.

Atmospheric
Chemistry
and Physics
Discussions

1020
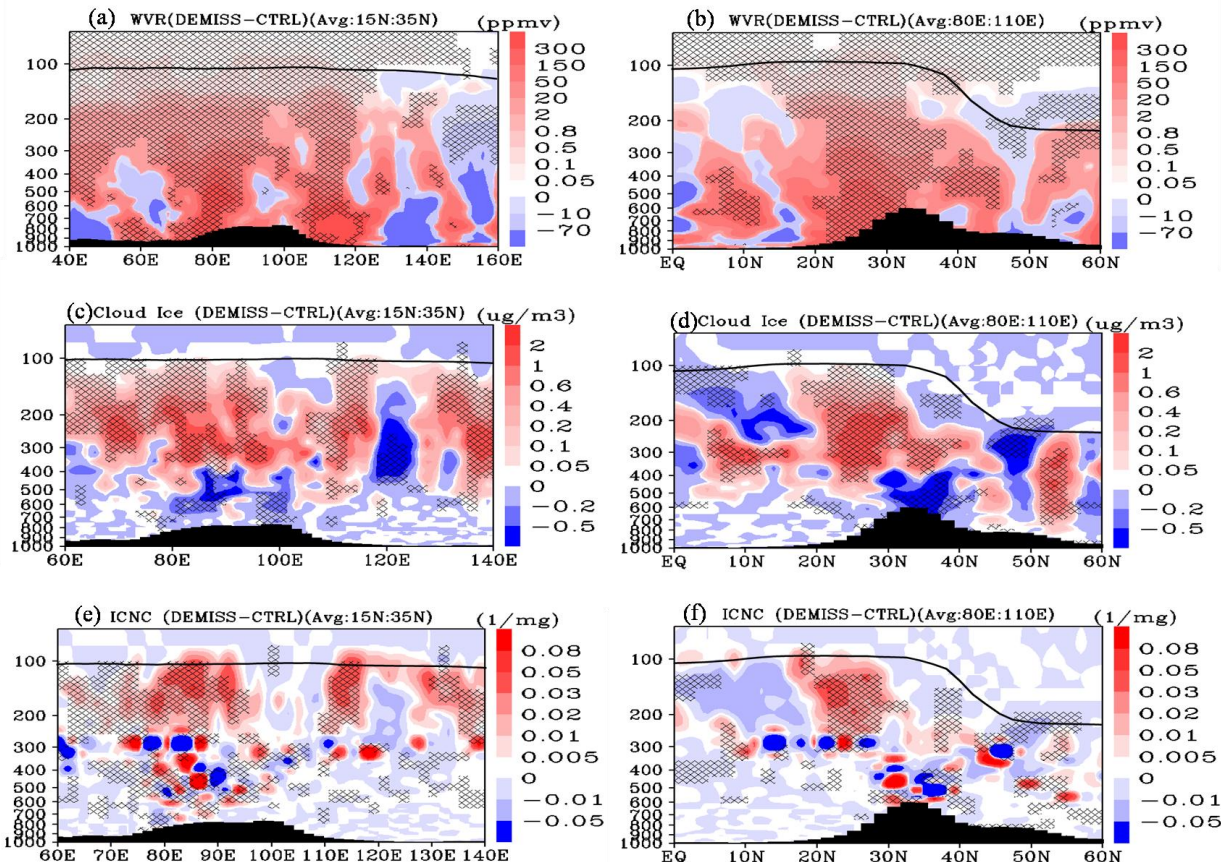
1021

Figure 6: Distribution of anomalies (DEMISS-CTRL) of water vapour (ppmv) averaged for the monsoon season, (a) longitude-pressure cross section (averaged over 15°N - 35°N) (b) latitude-pressure cross section (averaged over 80°E - 110°E), (c) and (d) same as (a) and (b) but for cloud ice (μg/m^3) and (e) and (f) for ice crystal number concentration (ICNC) (1/mg). The thick black line shows the tropopause while black hatched lines indicate 99% confidence level. The tropopause is averaged over 15°N -35°N for Figs. (a), (c), (e) and over 80°E-110°E for Figs. (b), (d) and (f).

1029
1030